VOL. 14 No. 11, pp. 313-344 MAY 1953

Philips Technical Review

DEALING WITH TECHNICAL PROBLEMS
RELATING TO THE PRODUCTS, PROCESSES AND INVESTIGATIONS OF
THE PHILIPS INDUSTRIES

EDITED BY THE RESEARCH LABORATORY OF N.V. PHILIPS' GLOEILAMPENFABRIEKEN, EINDHOVEN, NETHERLANDS

A DECADE COUNTER TUBE FOR HIGH COUNTING RATES

by A. J. W. M. VAN OVERBEEK, J. L. H. JONKER and K. RODENHUIS.

621.385.832:621.318.57

Mechanical, electromagnetically operated counting devices which count the applied number of electrical pulses, have been known for a long time. In recent years there has been an ever increasing demand for counting devices which operate at a much higher speed. This demand exists both in telecommunication and for modern computers, for measuring frequencies and for carrying out nuclear measurements. It is only by electronic means that a solution is offered in these cases.

A new electronic tube, the E1T, which has been specially designed for counting purposes, can count pulses at a very high rate. The number of counts can be read directly on the tubes themselves.

There are various types of mechanical counting devices which are operated by an electromagnet under the influence of electrical pulses. With some of these the number of pulses can be read in figures, such as with counters for telephone calls; with others a switch lever is moved a number of steps equal to the number of pulses received, so that a given connection is established, as in the case with selectors in a telephone exchange. Due to the delay in build-up and die-away of a magnetic field and the inertia of the moving parts, the counting rate of such electromechanical counters is not very high. For computers which must make thousands of additions per second, for the pulse code systems used in telecommunication, etc., this rate is quite insufficient.

Electronic tubes have, of course, been widely used for counting purposes. With valves of the conventional type, however, fairly large numbers of valves are required. A further problem is to render the counted number visible.

Reports on the development work carried out by Philips in the field of electronic valves designed for switching have been published both in this review [1]) and elsewhere [2]). One of the tubes which has resulted from this research work is the decade counter tube. This tube has already been mentioned in the publications referred to in footnote [2]); a description of this tube is now given and a new circuit is discussed.

Description of the decade counter tube

The counter tube is provided with an electron gun which emits an electron beam towards the envelope of the tube. A deflecting device with a feedback system, which is to be discussed later, ensures that the beam can occupy ten discrete positions. The envelope is lined with fluorescent material which fluoresces at a different place for each of the positions, so that the position of the beam can be read from the figures 0, 1, 2,.....9 placed opposite the fluorescing marks (*fig. 1*). Before counting starts, the beam occupies position 0, after the first pulse it is advanced to position 1, after the second pulse to position 2, etc., until position 9 is reached. At the tenth pulse the beam is reset to position 0, and at the same time a pulse is fed to a second counter tube, as a result of which its beam is moved from position 0 to position 1.

[1]) J. L. H. Jonker and Z. van Gelder, New electronic tubes employed as switches in communication engineering, Philips tech. Rev. **13**, 49-54 and 82-89, 1951/52 (Nos 3 and 4).

[2]) J. L. H. Jonker, Valves with a ribbon-shaped electron beam: contact valve; switch valve; selector valve; counting valve, Philips Res. Rep. **5**, 6-22, 1950. J. L. H. Jonker, A. J. W. M. van Overbeek and P. H. de Beurs, A decade counter valve for high counting rates, Philips Res. Rep. **7**, 81-111, 1952 (No. 2).

Fig. 1. The E1T decade counter tube. A blue fluorescent mark indicates the figure which corresponds to the position of the electron beam in the counter tube, i.e. to the number of pulses counted.

This second tube therefore counts the decades. A third tube can be added which counts the hundreds, a fourth which counts the thousands, etc. (*fig. 2*). With n tubes in cascade it is thus possible to count up to $10^n - 1$ ($\approx 10^n$) pulses.

Fig. 3a shows a cross-section of the decade counter tube, whilst fig. 3*b* shows the diagrammatic representation which will be used in circuit diagrams. The cathode is of the conventional type as used in receiving valves, apart from the fact that it emits electrons from one side only of its rectangular cross-section. A control grid (g_1), four rod-shaped focusing electrodes (p_1, p_2) and an accelerating electrode (g_2), together with the cathode, form the electron gun. This has been so designed that the cross-section of the electron beam thus obtained is not circular but ribbon-shaped. As shown elsewhere [1,2]), a ribbon-shaped electron beam has the following advantages:

1) It is easy to obtain a fairly strong beam current at a relatively low voltage, for example 1 mA at 300 V.
2) The dimensions of the tube can be kept small, roughly as those of a normal receiving valve. The E1T counter tube (fig. 1) has a maximum diameter of 37 mm and a maximum height of 83 mm.
3) It is necessary to align the electrodes, which are fixed between two mica discs as in the technique used for manufacturing receiving valves, in one dimension only, namely in the direction normal to the plane of the beam; with a beam having a circular cross-section it would on the other hand be necessary to align the electrodes in two directions, which would render manufacture much more difficult.

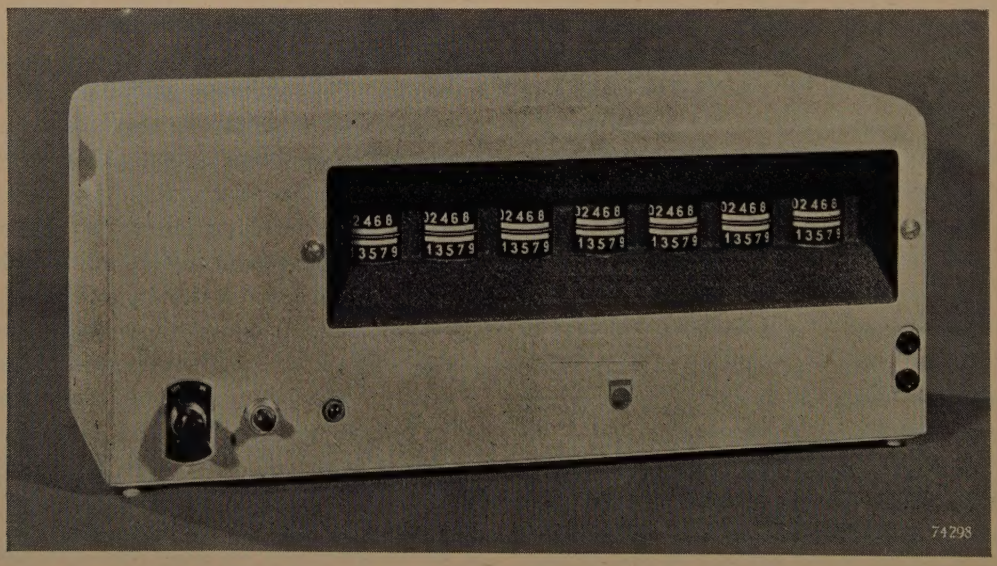

Fig. 2. Decade counter with seven decade counter tubes E1T connected in cascade, suitable for counting up to ($10^7 - 1$) at a speed of 30,000 pulses per second. From left to right the millions, the hundred thousands, the ten thousands, etc. can be read on the tubes themselves.
Bottom left: mains switch, push-button switch with which all counter tubes can be reset to zero before counting starts, and pilot lamp.
Bottom right: input terminals.

The importance of the advantages mentioned under (1) and (2) can be stated as follows. The advantage of a strong current in the case of a counter tube is related to the counting rate. Generally speaking, the time required for an "electronic event" is proportional to VC/I, where V is the potential difference traversed by the electrons, I the current intensity and C the inter-electrode capacitance. In order to keep this time short, it is thus favourable that V is kept small, I being given a large value. The ribbon shape of the beam is advantageous in both respects. Since C is proportional to the linear dimensions of the electrode system, attempts must moreover be made to keep this system small, i.e. to apply the technique used for receiving valves. It will be clear that the resulting small external dimensions of the tube are welcome also with a view to saving space.

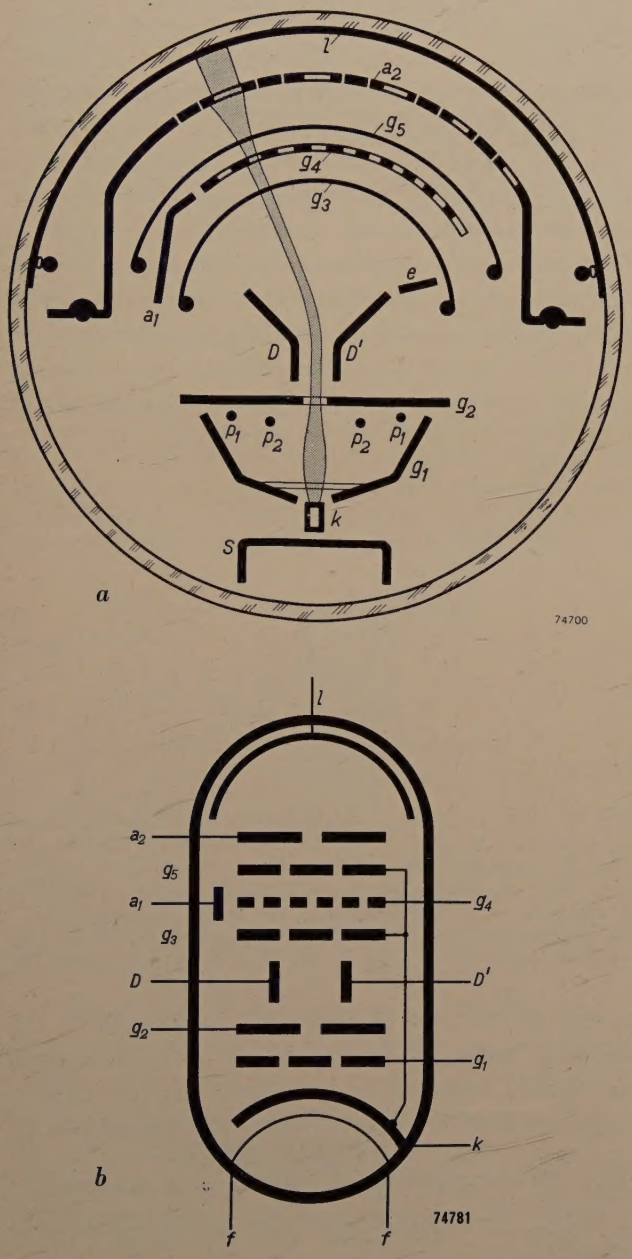

Fig. 3. (*a*) Cross section and (*b*) diagrammatic representation of the decade counter tube. The cathode k (with heater f), the control grid g_1, the four internally connected focusing electrodes p_1 and p_2 and the accelerating electrode g_2 form the electron gun, which produces a ribbon-shaped electron beam (the width of the ribbon is normal to the plane of the drawing). D, D' deflection electrodes. g_3, g_5 suppressor grids. a_1 reset anode. g_4 electrode with ten slots. a_2 anode. l fluorescent layer applied to a conductive layer. Screen s (internally connected to k) prevents primary electrons from impinging on the envelope. Auxiliary anode e (internally connected to g_2) captures secondary electrons.

The ribbon-shaped beam thus obtained proceeds between two deflection electrodes (D, D', fig. 3). These have been so positioned that the beam almost touches one of these electrodes in each of its extreme positions, deflection sensitivity thus being at a maximum.

At given values of the deflection, the beam passes through one of the ten vertical slots in the slotted electrode (g_4), which is at a positive voltage. It will be shown later how a special circuit ensures that the beam can occupy only one of these ten positions. Some of the electrons passing through a slot impinge on the anode (a_2) placed behind the slotted electrode; the remainder pass through an aperture in this anode and impinge on the envelope. The part of the envelope situated behind the anode is lined with fluorescent material, so that a fluorescing mark is produced behind the opening in the anode through which electrons pass. The number (fig. 1) opposite this mark thus indicates the position of the beam.

When the beam passes through slot *9*, it has not yet reached its extreme position, but can be deflected slightly further under the influence of a following pulse. When this occurs, it impinges on the so-called reset anode (a_1). The impinging of the beam on the reset anode initiates the resetting to position 0. Before discussing this, it will be shown how the beam is fixed at well-defined positions.

Step-wise deflection of the beam

Fig. 4a gives a schematic representation of an imaginary cathode-ray tube, containing an electron gun, a set of deflection electrodes and an anode. When the potential v_D of the one deflection electrode is kept constant and the potential $v_{D'}$ of the other is varied, the electron beam will move along the anode, but the anode current i_a remains constant (line I in fig. 4*b*). When the deflection electrode D' is connected to the anode and these two electrodes are fed via a common resistor R_a from a battery with voltage V_B (fig. 4*c*), the following equation, however, applies:

$$v_{a2} = v_{D'} = V_B - i_a R_a. \quad . \quad . \quad . \quad . \quad (1)$$

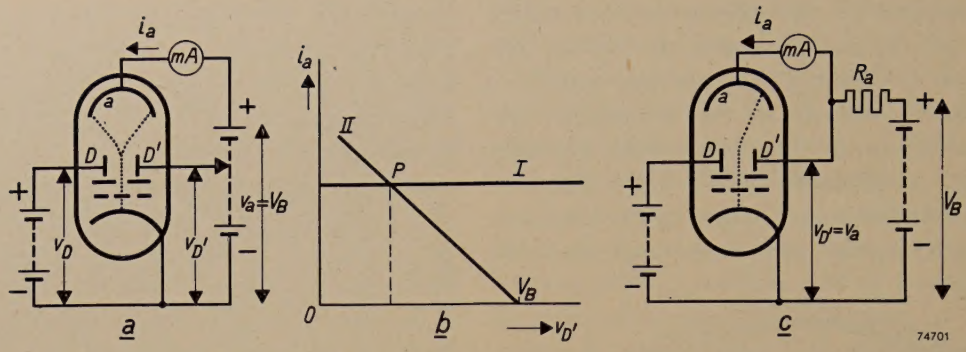

Fig. 4. (*a*) Imaginary cathode-ray tube with an electron gun, deflection electrodes D, D' and an anode a. At v_a and v_D = constant, the electron beam can be given any position between the extreme positions (dotted lines) by varying $v_{D'}$. In doing so the anode current i_a remains constant, see I in (*b*).

(*c*) When D' and a are connected to the positive terminal of a battery with voltage V_B via a common resistor R_a, eq. (1) is applicable (represented by the line II in (*b*). The beam can now occupy one position only, determined by the abscissa of the point of intersection P.

This relation is represented by the line II in fig. 4*b*. The point of intersection P of the lines I and II gives the state of equilibrium; the electrode D' then assumes a potential which corresponds to the abscissa of P, and according to this given potential the beam occupies a well-defined position.

Advantage is taken of this principle for fixing the positions of the beam in the counter tube. In this case too, the anode a_2 and the deflection electrode D' (i.e. the one nearest to the figure 0) are connected to a direct voltage source V_B via a common resistor R_{a2} (*fig. 5*); the potential of D and a_2 is denoted by $v_{D',a2}$. The straight line I of fig. 4*b* is now, however, replaced by the undulated curve I of *fig. 6*; the way in which this is obtained will be shown presently. This curve I is intersected 19 times by the resistance line II. Each of these points of intersection corresponds to a condition of equilibrium — although only the ten points of intersection numbered from *0* to *9* represent stable positions. From this it may be seen that the position of the beam indicated diagrammatically in fig. 3*a* is one of its stable positions, i.e., passing partly through a slot and impinging partly on the metal at the left of this slot: in fact, when the beam is deflected further to the left the current i_a initially decreases, in accordance with the characteristic I near the points of intersection *0*...*9* (*fig. 6*).

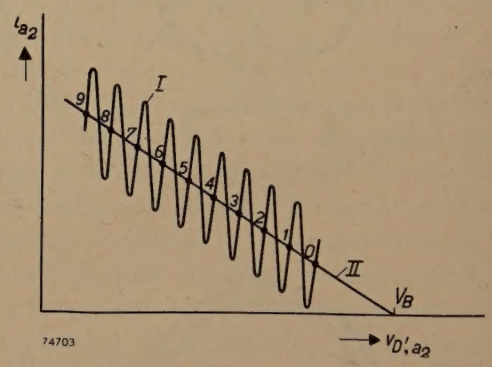

Fig. 6. The $i_{a_2}=f(v_{D',a_2})$ characteristic of the decade counter tube has the form of the undulated curve I. The straight line II represents the resistance line according to eq. (1). Only the points of intersection of I and II numbered from *0* to *9* represent stable positions of the beam; the other points of intersection correspond to unstable positions. V_B is only slightly larger than the abcissa of the point of intersection *0*.

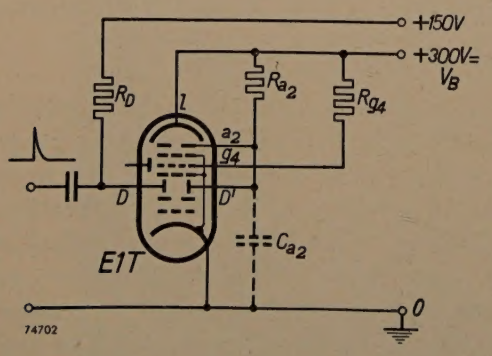

Fig. 5. E1T counter tube of which the anode a_2 and the deflection electrode D' are fed via a common resistor R_{a_2}, similar to the tube shown in fig. 4*c*. The beam has now the same number of stable positions as the number of slots in the electrode g_4 (see also fig. 6). By applying positive pulses to D, the beam can be advanced in steps (see later). C_{a_2} represents the stray capacitance.

How the characteristic $i_{a2} = f(v_{D',a_2})$ is obtained

In *fig. 7a* a slotted electrode and an anode have been drawn as flat planes. It is assumed that the ten slots have the same dimensions and are equidistant and that the thickness of the ribbon-shaped beam exceeds the width of the slots and is less than the width of the spaces between the slots.

When the beam is now made to move from slot *0* to slot *9* by (continuously) lowering the voltage v_{D',a_2}, it might be expected at first sight that a characteristic $i_a = f(v_{D',a_2})$ as shown by curve I

of fig. 7*b* is obtained: each time the beam is directed on a slot, i_{a_2} reaches a maximum (which has the same value for all slots), and each time the beam points to the centre between the slots, i_{a_2} drops back to zero.

Assuming for the time being that the characteristic had this form, it would be possible to proceed according to fig. 5, and to give V_B and R_{a_2} such values that the line *II*, which represents eq.(1) graphically, intersects all waves of *I* (fig. 7*b*). In practice, however, with a slotted electrode according to fig. 7*a*, the characteristic $i_a = f(v_{D'}, a_2)$ will not assume the form *I* of fig. 7*b*, but that of fig. 7c. The disadvantages of the latter form are that the magnitude of R_{a_2} (the slope of line *II*) must remain within very narrow limits and that V_B must be given a much higher value to prevent one or several points of intersection from being obliterated at the left-hand side. The form of *I* as shown in fig. 7*c* is a result of the asymmetry in the deflection (v_D constant, $v_{D'}$ variable).

It is in fact due to this asymmetry that the focusing of the beam on the slotted electrode deteriorates and that the beam thus becomes wider as it is displaced further to the left. Consequently, the number of electrons per second passing through the slots having high numbers is smaller than that passing through the slots with low numbers, i.e. the peaks of i_{a_2} become lower as the beam travels from the right to the left. The influence of the defocusing on the minima is even more serious because the beam soon becomes so wide when it is deflected that it is wider than the space between the slots. Consequently, as the beam moves towards the left, the current minima become less pronounced, i.e. the amplitude of curve *I* decreases towards the left.

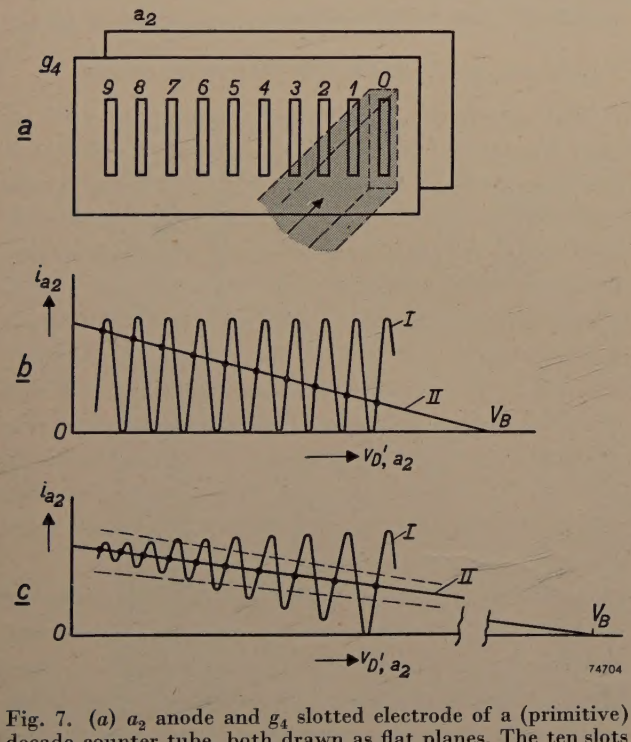

Fig. 7. (*a*) a_2 anode and g_4 slotted electrode of a (primitive) decade counter tube, both drawn as flat planes. The ten slots have been drawn as being of the same size and equidistant. (*b*) Curve *I*: $i_{a_2} = f(v_{D'}, a_2)$ characteristic which might be expected in the case (*a*). *II* again represents the resistance line. (*c*) Due to the defocusing of the beam as it is deflected to the left, the $i_{a_2} = f(v_{D'}, a_2)$ characteristic actually assumes the form represented by *I*. At small variations of R_{a_2} (corresponding to the broken lines) some of the points of intersection at the left are lost. V_B must, moreover, largely exceed the value of $v_{D'}, a_2$ corresponding to the point of intersection *0*.

In order to obtain the much more favourable characteristic *I* of fig. 6, the slotted electrode has been provided with additional apertures, which are also scanned by the beam, so that an additional current is passed which increases as the beam proceeds further to the left.

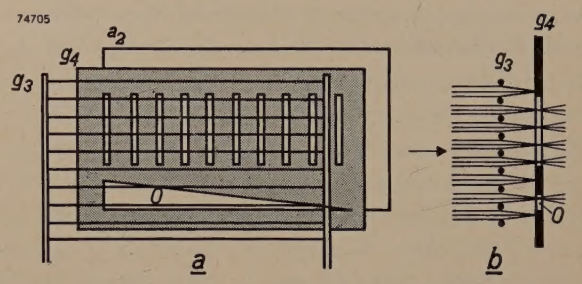

Fig. 8. (*a*) In order to obtain the characteristic *I* of fig. 6, the electrode g_4 might be provided with an additional triangular aperture *O* through which an additional current passes which increases as the beam is deflected further to the left. Due to the action of the suppressor grid g_3 (see the cross-section *b*), the magnitude of the additional current, however, depends too much on the location of g_3 with respect to the aperture *O*.

The most obvious solution is to make a triangular aperture in the slotted electrode (*O* in *fig. 8*). It would nevertheless be very difficult to obtain the desired improvement in this way. This is due to the presence of a suppressor grid (g_3) in front of the slotted electrode. The horizontal wires which constitute this grid give rise to a vertical variation of the current density of the beam with minima behind the grid wires and maxima behind the spaces of the wires (see fig. 8*b*). The "ribbon" might thus be imagined to be sliced into a number of threads situated above each other. The positions of the grid wires with respect to the narrow triangular aperture largely determine the way in which the current flowing through this aperture varies as a function of the deflection angle. This leads to difficulties in manufacture.

For this reason the idea of a narrow triangular aperture was abandoned in favour of rectangular apertures whose positions with respect to the grid wires are less critical. As shown in *fig. 9*, part of the beam passes through an aperture O_1 from slot 5 onwards. In positions 8 and 9 a second aperture moreover becomes operative (O_2).

A second measure applied to obtain a rising characteristic consists in making each slot slightly larger than its predecessor: starting from *2* to *9* the width gradually increases, whilst *1* is slightly lower than *2*....*9*. Slot *0*, which is made particularly wide, forms an exception, the reason of which will be shown later. To prevent the beam from bending around the edge of this wide opening — which might result in the figure 1 being indicated — slot *0* is covered with gauze.

By these measures the characteristic assumes the form as depicted [3]) in *fig. 10*. Due to the rising characteristic, V_B need not be much higher than the value of v_{D',a_2} at which the beam occupies position 0. A value of $V_B = 300$ V suffices; as will be seen from a circuit diagram to be discussed later, all other direct voltages the tube requires can be derived from the same source. The value of R_{a_2} should be approximately equal to the average slope of the characteristic, which amounts to about 1 MΩ,

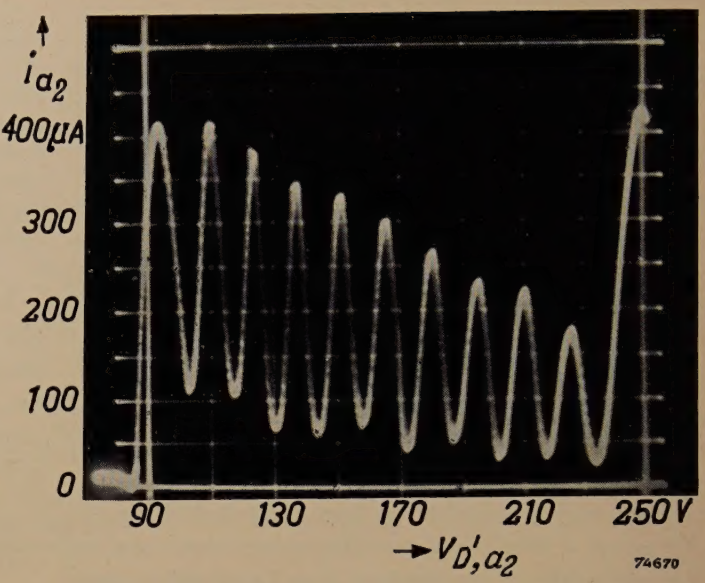

Fig. 10. Oscillographically [3]) plotted $i_{a_2} = f(v_{D',a_2})$ characteristic of the E1T counter tube. Cf. curve *I* shown in fig. 6. The oscillogram displays one peak more than the theoretical curve shown in fig. 6. This is due to the fact that in practice a peak — the one the extreme left — also occurs when the beam passes between the slotted electrode and the reset anode. This peak is of no consequence for the operation of the tube.

but owing to the large amplitude of the waves there is a reasonable play in the magnitude of R_{a_2}, although it remains desirable to keep the deviation within 1% for other reasons.

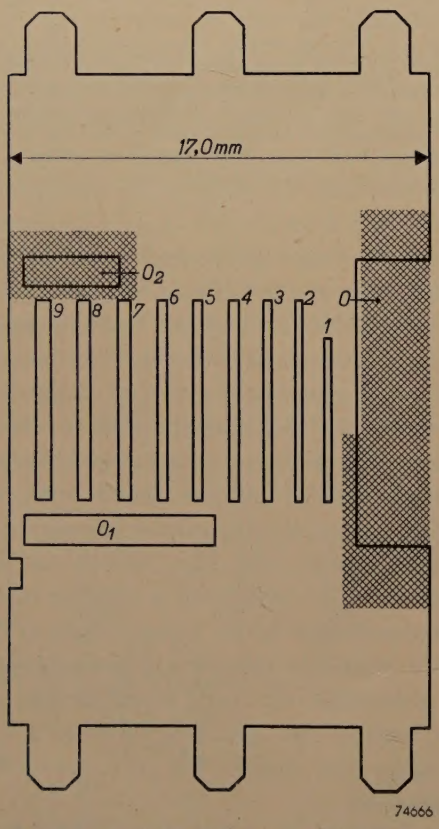

Fig. 9. Actual form of the apertures in the slotted electrode g_4 (drawn as a flat plane). The slots become larger and their distances from centre to centre increase in the sequence from *1* to *9*. An additional current passes through the two apertures O_1 and O_2 of which the upper one, like slot *O*, is covered with gauze.

Suppressor grids, anode and fluorescent screen

The previously mentioned suppressor grid g_3 (fig. 8) serves for rejecting secondary electrons which are emitted by the slotted electrode and would otherwise proceed mainly towards the deflection electrodes. A small proportion of these electrons, however, still passes through the suppressor grid, which is particularly troublesome when the beam is in position 0 or 1. For this reason an auxiliary anode has been incorporated at the right-hand side (*e* in fig. 3*a*); a voltage of 300 V is applied to this auxiliary anode, so that it captures these electrons. The screen *s*, which is mounted behind and connected to the cathode, prevents primary electrons from impinging on the envelope.

A second suppressor grid (g_5, fig. 3) is mounted between the slotted electrode and the anode and decelerates secondary electrons originating from the anode. It moreover "reassembles" the beam of primary electrons, which was sliced into threads by the first suppressor grid (fig. 8*b*), so that the ribbon-shaped beam again becomes homogeneous once it has passed the second suppressor grid [4]) (*fig. 11*). If this were not the case, the electrons which

[3]) Plotted with an apparatus as decribed in Philips tech. Rev. **12**, 283-292, 1950/51.

[4]) J. L. H. Jonker and B. D. H. Tellegen, Philips Res. Rep. **1**, 12-19, 1945.

pass through one of the ten slots of the anode would no longer give rise to a uniformly luminescing spot, but would produce a less distinct, "crumbly" spot.

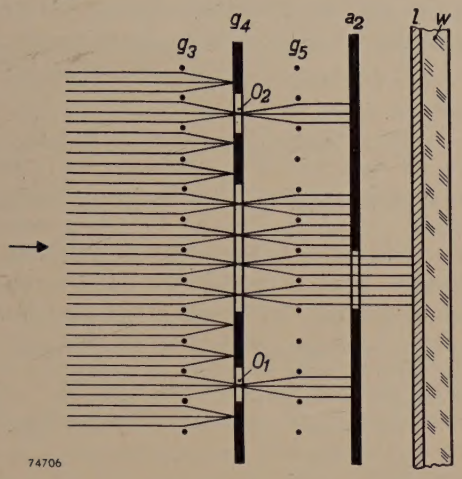

Fig. 11. Cross-section through the first suppressor grid g_3, the slotted electrode g_4, the second suppressor grid g_5, the anode a_2, the fluorescent layer l and the glass envelope w. By giving g_5 the correct pitch and position, a homogeneous beam is restored behind g_5.

By giving the grid g_5 the same pitch as g_3 and positioning it so that its wires are situated in the same horizontal planes as those of g_3, the beam will once again be homogeneous (fig. 11).

The fluorescing layer consists of a specially prepared type of zinc oxide with blue fluorescence and a very long life. It is applied to a conducting layer, which, during operation, is at a potential of 300 V.

In order to facilitate reading of the figures, they are placed in two rows above each other: 0....8 and 1....9 (fig. 1). The apertures in the anode are placed at corresponding positions; see *fig. 12*, in which the various parts of the tube are shown.

Mechanism of the displacement of the beam from 0 to 9

The positive-going voltage pulses to be counted are applied to the left deflection electrode D via a blocking capacitor, as shown in fig. 5.

In order to understand how the beam is shifted to a following position at each pulse, it should be recognized that the characteristic I shown in fig. 6 is applicable to a constant voltage v_D at the left deflection electrode, and that the angle of deflection is a function of $v_{D'} - v_D$. An increase of v_D by an amount V_i therefore corresponds to the line I being shifted to the right over a distance corresponding to V_i (*fig. 13*).

As a starting point it is assumed that the beam occupies one of its stable positions, for example

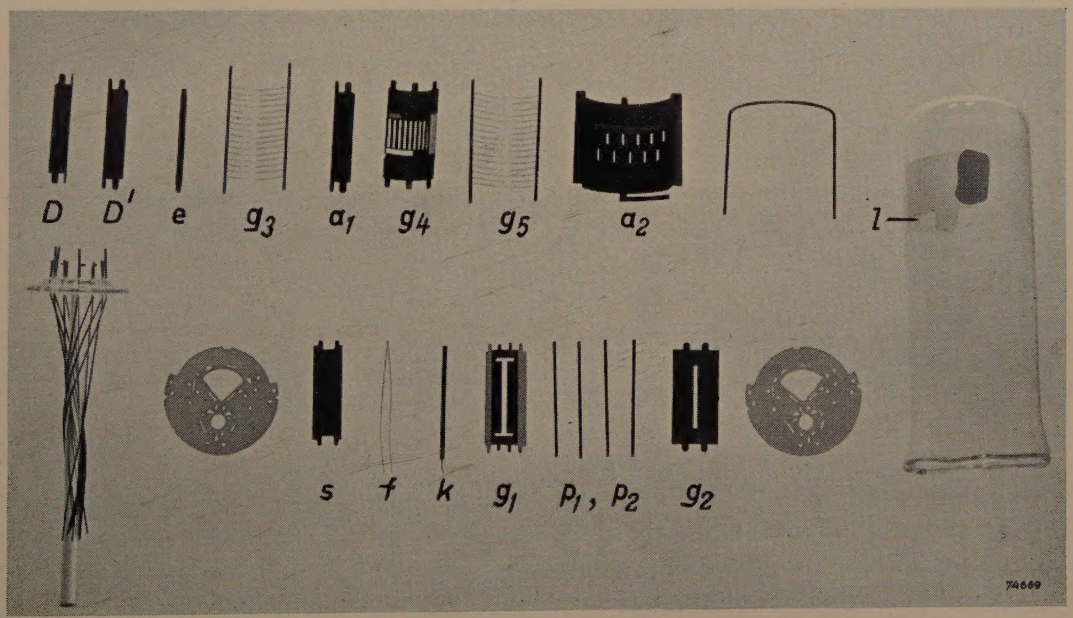

Fig. 12. Component parts of the E1T counter tube. The references have the same meaning as in fig. 3.

Lower row from left to right: glass base with pumping stem, mica support, screen (s), heater (f), cathode (k), control grid (g_1), four focusing electrodes (p_1, p_2), accelerating electrode (g_2), second mica support.

Upper row, from left to right: the two deflection electrodes (D, D'), auxiliary anode (e), first suppressor grid (g_3), reset anode (a_1), slotted electrode (g_4), second suppressor grid (g_5), anode (a_2), resilient bracket (to establish contact with the conductive layer on the envelope), envelope with fluorescent layer (l).

position 0. If a positive pulse is now applied to the left deflection electrode, so that v_D is temporarily increased, the beam will tend to move to the left (fig. 3*a*); the number of electrons passing through

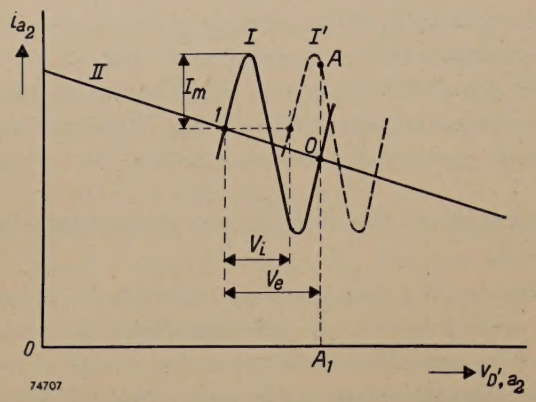

Fig. 13. $i_{a_2} = f(v_{D',a_2})$ characteristic I of the counter tube for a given voltage v_D on the left deflection electrode; I' the same characteristic for a voltage $v_D + V_i$ on the left deflection electrode. II resistance line. I_m amplitude of the waves. V_e horizontal distance between two adjacent stable points of intersection.

slot *0* then decreases, i.e. the anode current i_{a_2} is reduced. If no stray capacitances were present, the decrease of i_{a_2} would result in a rise of the potential of the anode and of the right deflection electrode connected to it, and this increase of v_{D',a_2} would counteract the deflection to the left, so that the beam would be retained at position 0.

In practice, however, the stray capacitance to earth of the electrodes a_2 and D' and their wiring, represented by C_{a_2} in fig. 5, is shunted across R_{a_2} and impedes sudden changes of the potential of a_2 and D'. Provided the condition is satisfied that the leading edge of the pulse is sufficiently steep, the potential v_{D',a_2} may be considered constant during the rise time ϑ_1 of the pulse (*fig. 14*). This amounts to the line I of fig. 13 being shifted to the right (I') over a distance equal to the amplitude V_i of the pulse, the anode current thus assuming the value A_1A. This differs from the original value, whereas the current flowing through R_{a_2} still has its original value; the difference is supplied by the capacitance C_{a_2}.

Provided the second condition is also satisfied, namely that the decay time ϑ_2, during which the pulse decays from V_i to zero, is sufficiently long, the characteristic I' will gradually return to I, and A will be shifted to the adjacent stable point of intersection between I and II, i.e. point *1*. In order to ensure that the beam is shifted just one step to the left, a third condition must be imposed to the beam, namely that the amplitude V_i should be roughly equal to the voltage difference V_e which corresponds to the horizontal distance between two adjacent stable points of intersection and amounts to approximately 14 V; it will be clear that at too small an amplitude the beam will return to its original position, whereas at too large an amplitude it will be advanced two or more steps.

As a result of the deflection being asymmetrical, the average potential in the space between the deflection electrodes drops each time the beam is shifted a step further to the left, since v_{D',a_2} decreases and v_D remains constant. As a consequence the deflection sensitivity increases, i.e. the reduction of $v_{D'}$ corresponding to a given increase of the deflection is smaller at the left than at the right. In the case of the primitive slotted electrode shown in fig. 7*a*, with equidistant slots, this means that the distances between the points of intersection of I and II become smaller in the direction from the right to the left (see fig. 7*c*), hence that V_e decreases from the right to the left. This is undesirable as it decreases the tolerance in the amplitude V_i of the pulses. This objection has been met with by increasing the distances between the centres of the slots in the direction from 0 to 9 in such a way that the gradually increasing deflection sensitivity is exactly compensated.

In practice the conditions imposed on the pulse may be formulated as follows:

$$\text{Interval } \vartheta_1: \quad \frac{dv_i}{dt} \geqq 3\,\frac{I_m}{C_{a_2}}, \quad \ldots\ldots \quad (2)$$

$$\text{Interval } \vartheta_2: \quad -\frac{dv_i}{dt} \leqq 0.3\,\frac{I_m}{C_{a_2}}, \quad \ldots\ldots \quad (3)$$

where v_i denotes the instantaneous value of the pulse amplitude and t the time. Theoretically, it might be expected that the amplitude of V_i may assume a value between $\frac{1}{2}V_e$ and $\frac{3}{2}V_e$, but the margin becomes smaller due to several causes. In fact, the following condition is valid:

$$\left.\begin{array}{l} 11.5\ \text{V} < V_i < 16\ \text{V} \\ \text{or} \qquad V_i = 13.6\ \text{V} \pm 18\,\%. \end{array}\right\} \quad \ldots\ldots \quad (4)$$

When it is assumed that $I_m = 0.1$ mA and $C_{a_2} = 15$ pF, it can be calculated that v_i must

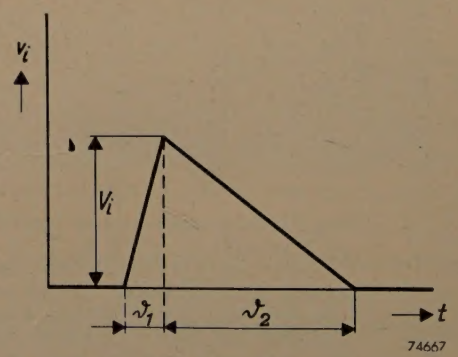

Fig. 14. Pulse voltage v_i as a function of the time t. V_i denotes the amplitude, ϑ_1 the rise time, ϑ_2 the decay time.

increase not slower than 20 V/μsec and subsequently decrease not faster than 2 V/μsec. At these extreme values of the slopes and $V_i = 14$ V, $\vartheta_1 = 0.7$ μsec and $\vartheta_2 = 7$ μsec.

If the counting pulses do not satisfy the imposed conditions they must be applied to a pulse shaper, i.e. a device which produces a pulse of the required form and amplitude for each pulse applied. Such a device will be referred to later.

Circuit for counting rates up to 30,000 per second

As previously shown, each tenth pulse applied to a counter tube should have two consequences: firstly the beam in the tube considered should be reset from position 9 to position 0, and secondly a pulse should be fed to the following counter tube to advance its beam one step. Both events are initiated by the fact that every tenth pulse initially deflects the beam occupying position 9 still further to the left, so that it leaves the slotted electrode and impinges on the reset anode.

The reset anode is connected to the +300 V line via a resistor, so that its potential (v_{a1}) depends on i_{a1}, i.e. on the extent to which it is struck by the beam. The variations of v_{a1} are now used for initiating the resetting and for ensuring that a pulse is passed to the following counter tube.

Several circuits have been designed for this purpose. On closer investigation some of these circuits appeared to have the disadvantage of being suitable only for fairly low counting rates, whilst others produce faulty counts when the resistors or capacitors deviate very slightly from the rated values or when a counter tube is replaced.

These objections are not applicable to the carefully investigated counter circuit described below; a practical example of a decade counter built on these lines is shown in fig. 2. This circuit is characterized by the fact that each counter tube is followed by a pulse shaper, which feeds a resetting pulse to the preceding counter tube and a counting pulse to the following tube. The first counter tube is, moreover, preceded by a pulse shaper (of a slightly different type) which is commonly used in counter circuits and serves for converting the initial pulses into pulses of the required form and amplitude. Both types of pulse shaper incorporate a double triode (E90CC), so that for n counter tubes $(n+1)$ E90CC tubes are required (see *fig. 15*).

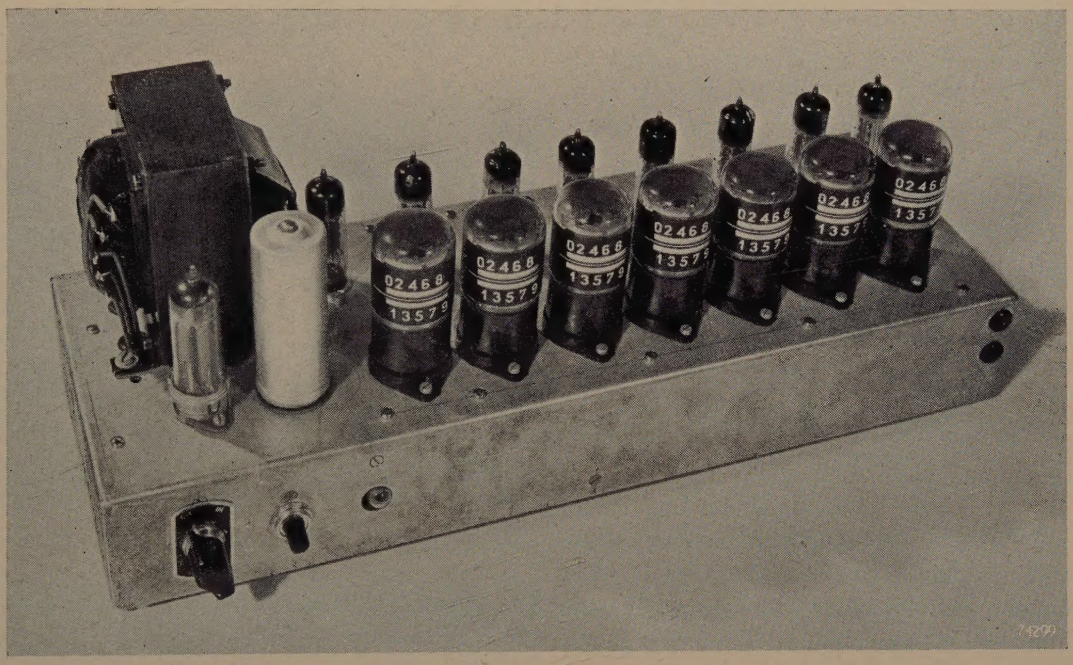

Fig. 15. The decade counter depicted in fig. 2 with the cover removed. Behind the seven E1T counter tubes the eight double triodes E90CC, which act as pulse shapers, can be seen. At the left is the rectifier valve AZ 41 which provides the direct current for the entire apparatus (300 V, approximately 50 mA).

The two types of pulse shaper will now be discussed separately.

Interstage pulse shaper

The pulse shaper which follows each counter tube is triggered each time it receives a pulse from

the reset anode of the preceding counter tube. It then feeds a counting pulse of the required form and amplitude to the following counter tube and, moreover, ensures that the current in the preceding tube is temporarily suppressed during a sufficient length of time to allow the anode voltage of this tube to rise to the value corresponding to position 0, after which the beam is restored.

Further details follow from the circuit shown in

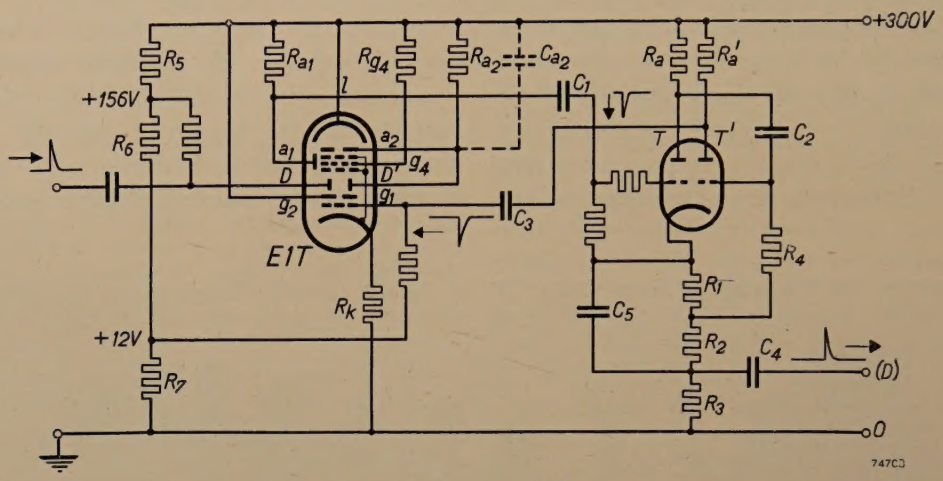

Fig. 16. Circuit of a counter tube and the following pulse shaper. The latter is a monostable (one-shot) multivibrator (flip-flop) incorporating a double triode T-T' (type E 90 CC).

At each tenth pulse applied to D the beam is advanced to a_1, which results in a negative pulse being fed to the grid of T via C_1. The multivibrator is thus triggered and brought from the stable condition (T conducting, T' cut off) into the quasi-stable condition (T' conducting, T cut off), but after a short interval it returns to the stable condition. During this operation two pulses are supplied: across R_3 a positive pulse is produced, which is fed to the following counter tube, whilst at the anode of T' a negative pulse is produced which is fed to the control grid (g_1) of the preceding counter tube; its beam is thereby temporarily suppressed and occupies position 0 after being restored.

R_a is the load resistor of T (39,000 Ω), R_a' is the load resistor of T' (3300 Ω).

fig. 16, in which one stage (counter tube and accessory double triode) is represented. The E90CC, in combination with a number of resistors and capacitors, forms a monostable ("one-shot") multivibrator, i.e. a multivibrator with one stable and one quasi-stable condition. The stable condition is that in which only triode section T passes current. When a negative voltage pulse is applied to the grid of T, this section is cut off and the other section, T', becomes conducting. From this quasi-stable condition the multivibrator automatically returns to the initial condition.

The operation of the monostable multivibrator may be explained as follows. The current which flows through T produces in the part R_1 of the cathode resistor ($R_1+R_2+R_3$), a voltage drop which acts as negative grid bias for T' and ensures that this section is cut off. The anodes and the grids of T and T' will be denoted by a and a', and g and g' respectively. When the current flowing through T is decreased by a negative pulse on g, the potential of a and thus also that of g' rises, since g' is coupled to a via a capacitor (C_2). Due to the potential rise of g', current starts to flow through T', and since the anode resistor of T' has a much smaller value than that of T (R_a' = 3300 Ω, R_a = 39,000 Ω), this current largely exceeds that which flowed through T. As a result of this larger current, the cathode potential rises to such an extent that T is completely cut off.

Meanwhile the coupling capacitor C_2 is charged. The charging current flows through the resistor R_4, thus producing a voltage drop which acts as a positive grid bias for T'. The charging current decreases exponentially, and so does the potential of g'. The cathode potential follows that of g' and after some time — depending on ($R_a + R_4$) C_2 — reaches the value at which T again becomes conducting. The potential of a then drops and so does that of g'. Section T' is cut off and C_2 is discharged via T, the stable condition thus being re-established.

The negative pulse which triggers the multivibrator is derived from the reset anode via a coupling capacitor (C_1). The potential of this anode obviously drops when it is struck by the beam.

The sudden voltage drop which occurs at the anode of T' when current starts to flow through T', is used for temporarily suppressing the beam in the counter tube (in this way also terminating the negative pulse by which the multivibrator was triggered). This is achieved by coupling the anode of T' via a capacitor (C_3) to the control grid (g_1) of the counter tube. This grid has normally a voltage of +12 V with respect to earth, derived from a voltage divider (R_5-R_6-R_7) between the +300 V line and 0. By reducing the voltage on g_1 to −15 V or

an even lower value, the beam is suppressed.

While the beam still occupies position 9 (anode current $= I_{a9}$), the anode potential of the counter tube is $V_{a9} = V_B - I_{a9}R_{a2}$. Now V_{a9} is the lowest of the various potentials $V_{a0} \ldots V_{a9}$ that the anode assumes in the positions 0...9 — as shown by the oscillograms of *figs 17a* and *b* — since I_{a9} is the largest anode current. As the resistor R_{a2}, shunted by the stray capacitance C_{a2}, is connected between the anode and the +300 V line, the anode potential v_{D',a_2} rises exponentially as soon as the anode current has become zero (as a result of the beam having been advanced to the reset anode and subsequently having been suppressed). The beam must be suppressed during such a length of time that V_{D',a_2} has sufficient opportunity to rise to a value which exceeds $V_{a0} = V_B - I_{a0}R_{a2}$, where V_{a0} and I_{a0} denote the anode voltage and anode current at position 0 of the beam. When the beam is now restored after the negative pulse on the control grid has ceased, the anode and the right deflection electrode have reached a potential which exceeds the potential corresponding to position 0. As a consequence the beam is deflected to the extreme right and from this position it automatically travels to the adjacent stable position, i.e. position 0. The resetting is thus completed.

a

b

Fig. 17. Oscillograms of the anode voltage v_{D',a_2} of the counter tube shown in fig. 16, as a function of the time t. (*a*) has been registered at 3000 and (*b*) at 30,000 pulses per second. In position 0: $v_{D',a_2} = V_{a0} = 240$ V; in position 9: $v_{D',a_2} = V_{a9} = 95$ V. Between 9 and 0 the beam is suppressed and v_{D',a_2} rises exponentially.

The same principle is used for resetting all counter tubes to zero before counting starts. By means of a press-button switch (fig. 2) a negative voltage is applied to all control grids g_1, as a result of which the beams are suppressed and occupy position 0 when they are restored. The circuit required for this purpose has been omitted in fig. 16.

Finally, the pulse which should be fed to the following counter tube will be dealt with. For this purpose the voltage drop is used which is produced across the part R_3 of the cathode resistor of T-T' when, owing to the multivibrator being triggered, a larger current starts to flow through T' than previously flowed through T. The pulse is applied to the left deflection electrode of the following counter tube via a coupling capacitor (C_4).

The slope of the leading edge of this pulse depends on the speed with which the multivibrator changes from the stable to the quasi-stable condition. If the capacitor C_5 were absent, the strong negative feedback caused by the presence of the cathode resistor ($R_1+R_2+R_3$) would delay the triggering of the multivibrator to such an extent that the pulse would not be steep enough. Large negative feedback is, however, necessary to ensure good stability (insensitivity to changes of the valve characteristic, etc.). To solve this difficulty, R_1+R_2 is by-passed by the capacitor C_5, the capacitance of which is so chosen that only the cathode resistor R_3 is operative for "rapid" changes, whereas the complete resistor ($R_1+R_2+R_3$) is operative for slow changes.

The cathode resistor (R_k) of the counter tube also serves for increasing the stability.

The circuit of fig. 16 occurs seven times in the decade counter depicted in fig. 15. This circuit may be built as a separate unit which can be plugged into a tube holder. In this way counters can easily be assembled. *Fig. 18* shows an example of such a unit [5]).

Amplitude and duration of the pulses; counting rate

The positive pulse supplied by the pulse shaper must satisfy the conditions (2), (3) and (4) formulated above: sufficiently high slope of the leading edge, sufficiently low slope of the trailing edge, and an amplitude of 13.6 V $\pm$ 18%. The negative pulse, see *fig. 19*, must be sufficiently large to suppress the beam during at least the time τ that is required by v_{D',a_2} to rise from the value V_{a9} to

[5]) This unit is not in production.

V_{a0}, but its duration should, on the other hand, not exceed τ considerably, since this would affect the counting rate.

The time τ is given by the following equation:

$$V_B - V_{a0} = (V_B - V_{a9})\, e^{-\tau/R_{a2}C_{a2}}.$$

By substituting $V_B = 300$ V, $V_{a0} = 240$ V, $V_{a9} = 95$ V, $R_{a2} = 1.05$ MΩ and $C_{a2} = 16$ pF in this equation, τ is found to be 21.3 μsec. Making allowance for a safety margin, the condition is imposed that the pulse must not be shorter than 23 μsec. Taking the same tolerance (±18%) for the pulse duration as for the amplitude, an average duration of 27.2 μsec is obtained, the extreme values being 23 and 32 μsec. Allowing another 1.3 μsec as a margin, the longest pulse duration corresponds to a maximum repetition frequency of $10^6/(32 + 1.3) =$ 30,000 pulses per second.

Fig. 18. A decade counter tube with its accessory pulse shaper connected according to the circuit of fig. 16, in the form of a unit [5]) to be inserted in a tube holder.

The conditions regarding the form, amplitude and duration of the pulse can be met by a suitable choice of the component values. The question remains, however, whether these conditions are still satisfied when these values are subject to slight changes. In the circuit of fig. 16, by way of experiment, all resistances were changed simultaneously by 2% and all capacitances by 5%; the sign of each change was such that the influence on the final result was a maximum. The change of the pulse duration proved to be 7.5% and that of the amplitude appeared to be 8%; both changes thus remain well within the tolerance of 18%.

Fig. 19. Oscillogram of the negative pulse with which the pulse shaper (fig. 16) temporarily suppresses the beam of the corresponding counter tube.

Input pulse shaper

As the original pulses which are to be counted do not, as a rule, satisfy the imposed conditions, the first counter tube must be preceded by a pulse shaper. It might be expected that the previously discussed multivibrator can be used for this purpose, but a closer investigation reveals that it is necessary to extend this circuit.

The interstage pulse shapers are triggered by negative pulses which are derived from the preceding counter tube (fig. 16); the duration of these pulses is but a fraction of 1 μsec, that is, much shorter than the duration of the output pulses (23-32 μsec). The pulse shaper at the input, on the other hand, is triggered by the original pulses, the duration of which may be considerably longer than 23 μsec, particularly so at low counting rates. For reliable operation a multivibrator requires triggering pulses of shorter duration than the pulses delivered.

This difficulty has been overcome by differentiating the original pulses by means of a capacitor C_d and a resistor R_d (*fig. 20*). If the form of the original pulse is, for example, as drawn in *fig. 21a*, a voltage will be produced across R_d, which — provided R_dC_d has been chosen small enough — approximates the form depicted in fig. 21*b*, remaining negative during a shorter length of time than the original pulse. The negative voltage is now, however, followed by a positive voltage which suddenly drops to zero at $t = t_2$. This sudden variation might trigger the pulse shaper again and give rise to a faulty count. This is why R_d is shunted by a germanium diode (fig. 20), which prevents the voltage across R_d from becoming positive.

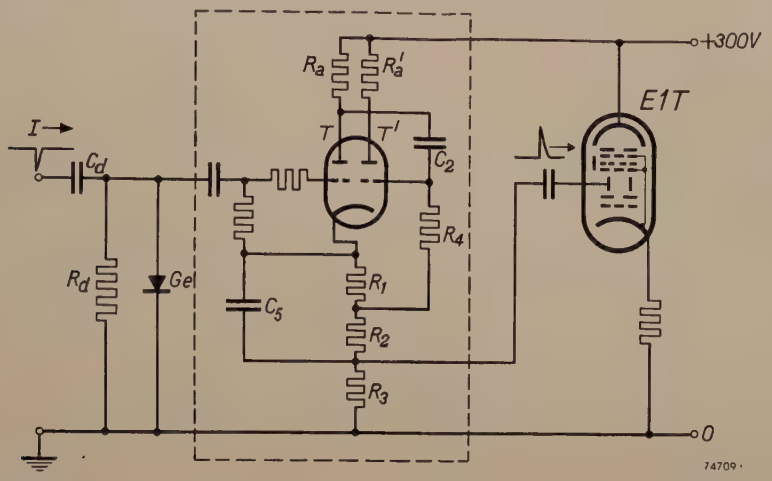

Fig. 20. Circuit of the input pulse shaper. *I* applied negative-going counting pulses. C_d-R_d differentiating network. *Ge* germanium diode (type OA 55), which prevents a positive voltage occurring across R_d. The circuit within the rectangle corresponds to that shown in fig. 16 of the other pulse shapers. At the right of this circuit is the first counter tube.

The input pulse shaper need supply pulses for operating the first counter tube only. The condition that the pulse duration must be greater than τ is not applicable to these pulses, so that it was possible to reduce the duration of these output pulses to 13.5 μsec.

It would lead too far to discuss the other (small) differences between this pulse shaper and the others, and it will suffice to quote the conditions which must be imposed to the original pulses (assuming these to have roughly a square wave-form):

Amplitude	20 V to 50 V,
Leading-edge duration	< 13.5 μsec,
Interval between end of one pulse and beginning of next	$\geqq 10$ μsec.

These conditions can as a rule easily be satisfied, and provided the values of the circuit components remain within certain tolerances, a counting rate of 30,000 pulses per second can be obtained with certainty.

All E1T tubes are tested at this counting rate; during these tests the pulse amplitude and the anode resistor are varied in order to guarantee reliable operation of the tubes in the circuit discussed at 30,000 pulses per second. This counting rate is however by no means the highest rate obtainable with the tube. In the laboratory it has proved possible to obtain counting rates of the order of 100,000 pulses per second and, by using a triode-hexode and a secondary-emission valve as

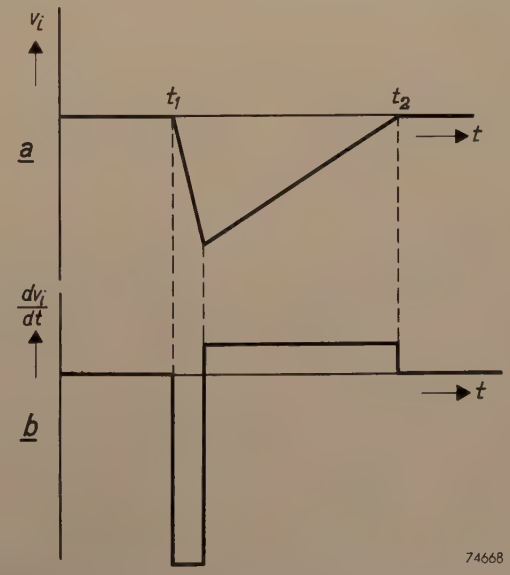

Fig. 21. Form of the original pulses (*a*) and of the pulses (*b*) after having been differentiated by C_d-R_d (fig. 20). The positive part in (*b*) is clipped by the germanium diode.

auxiliary valves, counting rates of millions of pulses per second have even been obtained [6]). For achieving these record performances the circuit parameters were adjusted to suit the individual tubes. On the other hand, the standard circuit discussed above will count up to 30,000 pulses per second without any special adjustment being made to allow for the unavoidable differences between production tubes.

[6]) See the second article quoted in footnote [2]).

Summary. A decade counter tube (E1T) has been designed which gives visual indication of the counts on the tube itself. The E1T is a cathode-ray tube — roughly the size of a receiving valve — whose electron gun produces a ribbon-shaped electron beam with a current of approximately 1 mA. A supply voltage of 300 V suffices for this tube. The beam impinges on an electrode with ten slots, behind which there is an anode with ten apertures. When the beam passes through a slot and an aperture, it impinges on a fluorescent layer with which the envelope is lined; at this spot a luminescent mark is produced adjacent to the corresponding figure (0.....9).

On its way from the gun to the slotted electrode the beam passes between two deflection electrodes. The slots and some auxiliary apertures in the slotted electrode are so dimensioned that the anode current as a function of the deflection voltage assumes a number of maxima and minima which increase as the beam is further deflected from 0 to 9. By feeding the anode and the one deflection electrode (that nearest to the figure 0) via a common resistor of suitable value, the beam is given ten stable positions of equilibrium, corresponding to the figures 0.....9. The beam is advanced to the following position by applying a positive pulse to the other deflection electrode.

At each tenth pulse the beam impinges on the reset anode. A suitable circuit ensures that the resulting voltage surge at this anode rapidly resets the beam to position 0, and, moreover, that a pulse is fed to the following counter tube, thus advancing its beam one step. The second tube thus counts the decades, and proceeding in this way, a third tube can be made to count the hundreds, a fourth tube the thousands, etc.

The slope and amplitude conditions which the pulses must satisfy are discussed. A circuit is outlined by means of which 30,000 pulses per second can be counted. In this circuit pulse shapers are used; the input pulse shaper converts the initiating pulses into pulses of the required form and amplitude, whilst the interstage pulse shapers initiate the resetting and feed a pulse to the following counter tube. All E1T counter tubes are tested at 30,000 pulses per second.

NEW DEVELOPMENTS IN THE IMAGE ICONOSCOPE

by J. C. FRANCKEN and H. BRUINING. 621.385.832:621.397.611

Although a description of the image iconoscope was given in this Review not long ago, it is now possible to publish details of two important improvements. One of these consists of the means of avoiding what is known as an ion spot or ion burn and, simultaneously, of reducing to a negligible degree a certain distortion in the electron-optical image. The other improvement refers to a new design of focusing coil which allows of continuous electrical control of the field of view without moving the camera. (This can be done optically only with the aid of very complicated lens systems.)

In Europe the image iconoscope is the most generally used camera tube for television. As explained in a previous article [1]), this tube performs its task — the conversion of the optical image or scene into an electrical signal — in three stages.

First the optical image is converted into a photo-emission image by means of the photo-cathode; in the second stage this image is reproduced in the target by an electron lens and, owing to the effect of secondary emission, a potential pattern is created on the target. Finally, a scanning device erases this potential pattern and simultaneously produces the video signal which is, in effect, the electrical translation of the original optical image.

The new development which is the subject of this article relates to the second stage, that is, the electron-optical projection of the photo-cathode onto the target. After mentioning an improvement in the internal design of the tube itself, which results in a much longer life and less distortion, an improvement to one of the accessories will be discussed which permits continuous variation of the electron-optical magnificaton.

Disadvantages of the ordinary electron lens

There are one or two disadvantages inherent in the ordinary type of electron lens, a full description of which was published in article I.

From the electron-optical aspect, the greatest defect is a certain amount of rotational distortion, although this in itself is not usually very noticeable. A more serious shortcoming originates in the form of the electrostatic field of the lens (see *fig. 1*). In the absence of a magnetic field, this electric field has the same effect as a negative lens and causes the paths of the emitted photo-electrons to diverge. Positive ions, however, which may be produced by impact between the photo-electrons and residual gases in the tube, are accelerated in the direction of the photo-cathode and their paths converge to form a spot of about 1 mm diameter in the centre of the cathode. Actually, the same thing happens when the magnetic field is present, as this is too weak to have any influence on the paths of the ions. In time, owing to this bombardement, the photo-sensitive layer is damaged and locally becomes less sensitive. An unpleasant dark spot is then visible in the televised picture, this being known as an ion spot.

So far, this has always been the factor that determines the life of the camera tube, and its occurrence depends upon circumstances which are very difficult to predict. In some tubes the spot becomes noticeable after several hundred hours' use, but there have been instances in which a tube has thus become useless after only 50 hours' service. The ion spot can be particularly annoying in outside programmes, especially sports events; the camera is then constantly moving and contrasts in the scene (e.g the sports ground) are usually quite low. The dark spot is then much more distracting than in programmes televised from the studio,

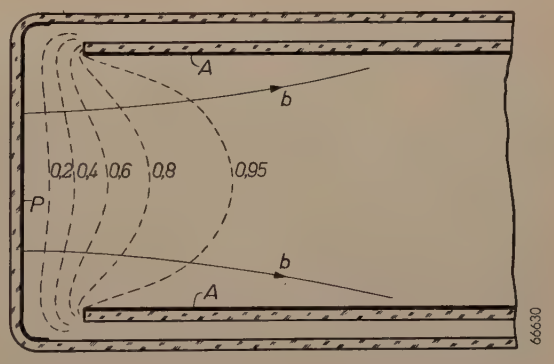

Fig. 1. Cross-section of the photo-cathode end of the old type of image iconoscope (type 5854/00). An accelerating electric field is present between the photo-cathode P and the anode A. Broken lines: equipotential planes (the potential of P is zero, that of A is taken to be unity).
b = electron paths in the absence of other fields.

[1]) P. Schagen, H. Bruining and J. C. Francken, Philips tech. Rev. **13**, 119-133, 1951 (No. 5), hereinafter referred to as article I.

where the camera is not moved so much and where the background (e.g. a back-drop), provides much greater contrasts.

Clearly then, there is an urgent need for obviating the occurrence of ion burn.

The use of a gauze

Both the defects mentioned can be remedied by closing the end of the anode cylinder with a very fine metal gauze (see *fig. 2*). This entirely removes

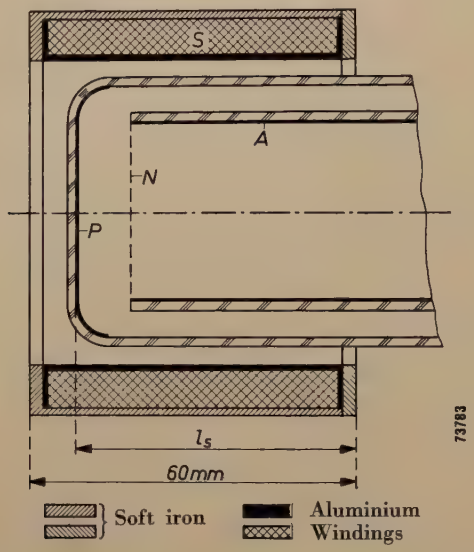

Fig. 2. Cross-section of the photo-cathode end of the improved image iconoscope (type 5854/02). P = photo-cathode. A = anode. N = fine metal gauze. S = focusing coil (diagrammatic).

the possibility of the occurrence of an ion spot. The electrostatic field between the photo-cathode and the anode is then uniform, and the positive ions are evenly distributed over the whole surface. In the long run the ion bombardment will still result in deterioration in the sensitivity, but the time involved before this happens will obviously be much longer than when bombardment is concentrated, as is the case with the field in its original form. Moreover, the image does not suffer in any way, since the decrease in sensitivity is uniformly spread over the whole area of the photo-cathode and is not manifested as a spot. Life tests have shown that there is no trace of an ion spot after several hundred hours' operation.

The question now arises what effect this modification in the electrostatic field will have on the quality of the electron-optical image (definition, magnification, distortion), as well as on the sensitivity.

Definition

On first thoughts it would appear that definition of the image would be bound to suffer, since the apertures in the gauze function as so many electron lenses. Experimentally, however, it has been found that there is no appreciable loss of definition in comparison with the old system, provided only that the mesh of the gauze is fine enough.

In the Philips image iconoscope (see article I) the limit occurs at a mesh of about 50 μ. The space between cathode and gauze is about 10 mm and the diameter of the particular cathode face is 20 mm.

Magnification

The magnification of the image differs from that obtained with a tube not fitted with the gauze. When the same coil is used for the two types of tube, the location of the photo-cathode in the magnetic field being the same in each case, the magnification is greater in the tube with the gauze (see *fig. 3*).

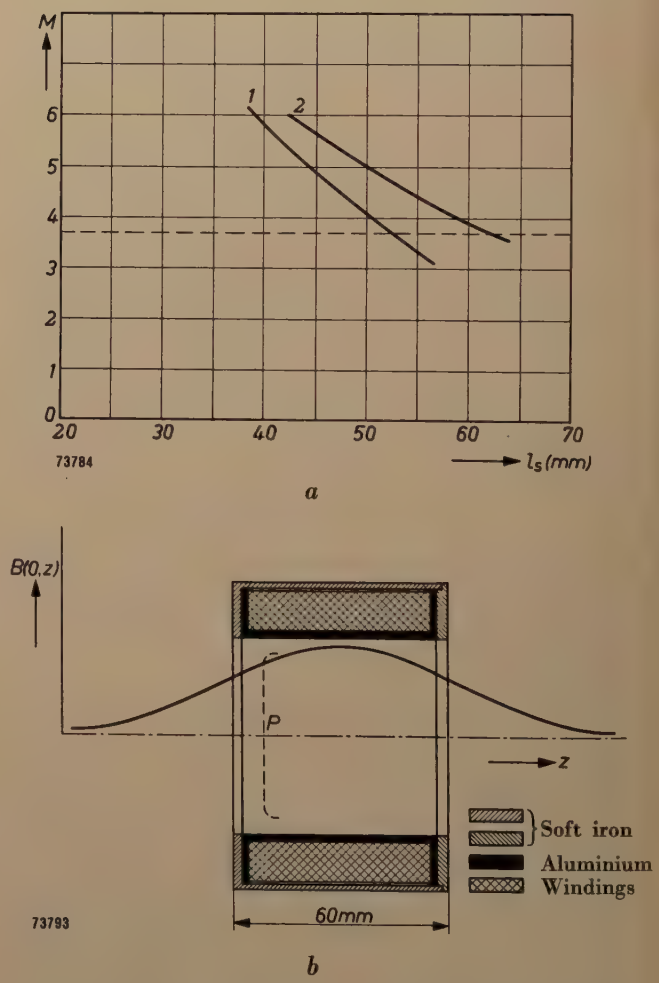

Fig. 3. *a*) Electron-optical magnification M of the image iconoscope type 5854 plotted against the distance l_s (see fig. 2). Curve *1* refers to the tube without gauze, curve *2* to the tube with gauze. The relevant focusing coil is shown in (*b*), in which the magnetic induction $B(0, z)$ along the axis (z) of the coil is also given. P = relative position of the photo-cathode.

In itself, this is a disadvantage, since from the point of view of sensitivity, it is important to keep the magnification in a given tube as low as possible. For a certain size of target the greatest possible area of the photo-cathode is then utilised, which means that higher sensitivity of the whole system can be achieved than if the effective area of the photo-cathode were small. (This will be explained in greater detail in a subsequent article dealing with the sensitivity of camera tubes.)

In the old type of image iconoscope (type 5854/00) an area of 12 mm × 16 mm of the photo-cathode was used. As the dimensions of the target were 45 mm × 60 mm, the magnification was 3.75×. In the tube with the gauze (type 5854/02) the same magnification can be obtained using the same coil by moving the latter nearer to the target end of the tube. As the electrons are now subjected to the magnetic field for a greater part of their travel, the magnification is decreased so that the magnifying effect of the gauze can be annulled (see fig. 3*a*). Under such conditions, however, considerable field curvature would result, in consequence of which the edges of the image are no longer sharp. As already pointed out in article I, this is due to the fact that the lines of magnetic force are then no longer perpendicular to the photo-cathode.

It was accordingly found necessary to design a new focusing coil for the tube containing the gauze, to give the desired magnification whilst retaining high definition at the corners. Dimensions for this coil were determined very simply from the experiments described below.

Rotational distortion

Theoretical considerations have led to the conclusion that the major source of rotational distortion is to be found in the vicinity of the photo-cathode, and it was somewhat surprising to find that this source of distortion originates mainly in a lack of uniformity of the electric field [2]).

In principle it should be possible to correct this defect by making the magnetic field non-uniform as well, viz. by making the magnetic field strength increase towards the edges. This idea has been worked out elsewhere [3]).

We have pursued another course, however, i.e. that of making the electric field uniform (by means of the gauze), this being at the same time, as already mentioned, an effective means of eliminating the ion spot.

The results, as far as distortion is concerned, obtained from a tube containing the gauze and fitted with the new coil, are demonstrated by the photographs shown in *fig. 4*. Fig. 4*a* was obtained from a tube without gauze, using the old type of coil.

[2]) J. C. Francken, Electron Optics of the Image Iconoscope, Thesis, Delft, 1953.

[3]) German Patent Applic. Class 21g 29/40 No. F 3126 and No. P 5137, published 28th February 1952 and 30th April 1952, respectively.

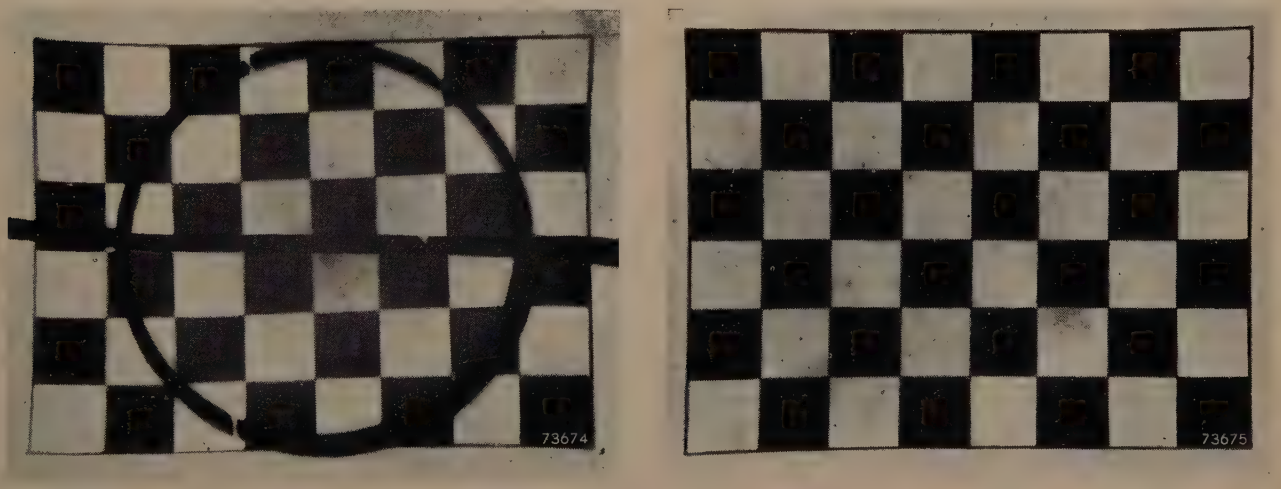

a *b*

Fig. 4. These photographs demonstrate the reduction in rotational-distortion when the electric field is rendered uniform:
a) with tube not fitted with gauze, and old type of coil;
b) tube with gauze, and coil as shown in fig. 12.
(In order that a direct observation might be taken, a fluorescent plate was mounted in each of the two tubes to take the place of the ordinary target. The fluorescent images produced on these plates are reproduced in the above photographs. The black circle and line in (*a*) are images of a figure applied to the photo-cathode for the purpose of measuring the magnification.)

It will be seen that the amount of rotational distortion inherent in the new design is very much less than before (fig. 4*b*). (It should be added that, even with the tube not equipped with gauze, less distortion results from the use of a coil similar to that designed for the tube with gauze. The results are, however, not quite as good as those obtained from the modified tube.)

Sensitivity

Lastly there is the question of the sensitivity of the new tube as compared with that of the tube without the gauze. The gauze unavoidably intercepts some of the photo-electrons, but a new process has made it possible to manufacture a very fine gauze with a ratio of aperture to material of 75 to 80%, which means that the loss in sensitivity is only some 25 to 20%.

Methods of varying the field of view

The production of T.V. programmes demands that at one moment a large part of a particular scene shall appear on the screen and at another only a small part of it; in other words that the field of view of the camera shall be variable. The means of achieving this may be either optical or electrical.

Optical means of varying the field of view

Optical variation is obtainable in the first instance by moving the camera closer to, or away from the scene. This facility, however, is effective only when the camera is already close to the scene, as is usually the case in the studio only.

The same effect can be produced by varying the focal length of the lens; the greater the focal length, the smaller the field.

This is explained in the following manner. Since the focal lengths in normal use are small compared with the object distance (camera to scene), the lens forms an image a very small distance beyond the focal plane, i.e. at a distance s' only slightly greater than the focal length f' (*fig. 5*). The field angle β is determined by:

$$\tan \beta = \frac{\frac{1}{2}d}{s'} \approx \frac{d}{2f'},$$

where d is the diagonal of the image. For a given value of d, therefore, a smaller field is obtained according as f' is increased.

In most T.V. cameras such variation in the focal length is obtained by means of a turret with 3 or 4 lenses of different focal lengths, a larger or smaller field being thus provided in steps, but a disadvantage of this system is that, when the lens is changed, the picture momentarily disappears; the usual practice, accordingly, is to switch over to another camera in the meantime.

Generally it is then unavoidable that the second camera picks up the scene from another angle, and the sudden change in direction and range tends to disturb the continuity of the action as seen on the receiver.

A much better effect is obtained by varying the focal length continuously and, in fact, lens systems have been developed, known as Zoom lenses, which are capable of such variation. They are, however, very heavy and the cost is extremely high. One such lens system [4]) is 75 cm (29″) in length and weighs 6.5 kg (14 lbs); another [5,6]) 48 cm long (19″), weighs 18 kg (40 lbs).

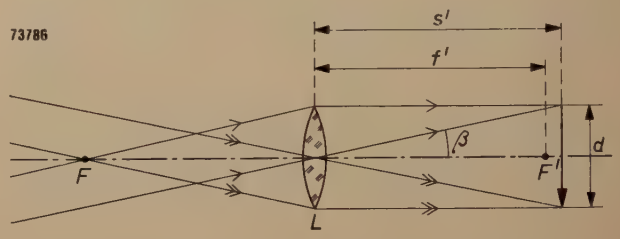

Fig. 5. The lens L, whose foci are F and F', forms an image of a remote object at a distance s' which is slightly greater than the focal length f'. β is the angle of view.

Electrical means of varying the field

The potential pattern on the target of the tube is scanned by a beam of electrons to produce the video signal. If the horizontal and vertical amplitudes of the scanning beam are reduced, only part of the image is transmitted and the field of view is thus reduced in size.

The advantages of this system are that, with only simple apparatus, it provides continuous control of the field of view, and that it can be applied to all current types of camera tube. It is a disadvantage, however, that when the field of view is reduced, the definition drops, owing to the fact that the cross-section of the scanning beam is independent of the amplitude; when the area scanned is reduced, the definition suffers.

With camera tubes such as the image iconoscope, which are operated with a scanning beam of high velocity electrons, there is the additional disadvantage that the secondary-emission coefficient of the area scanned is also somewhat affected. This is manifested as a sort of target burn when the reduced

---

[4]) R. C. A. Broadcast Equipment Catalog 1950, p. 206.
[5]) J. Opt. Soc. Amer. **41**, 863-864, 1951 (No. 11).
[6]) H. H. Hopkins, Television Zoom lens. Conv. British contribution to television, 1952, paper 1353.

scanning amplitudes are once more restored to their normal values, in that the rectangle originally scanned remains visible in the image.

In contrast with other camera tubes, image iconoscopes of the magnetic type — including the Philips model — offer facilities for varying the size of the field by other means, i.e. by varying the electron-optical magnification.

Electron-optical variation of the field of view

As already mentioned, a potential pattern 45 mm × 60 mm on the target of the Philips image iconoscope normally corresponds to an emission-image 12 mm × 16 mm on the photo-cathode; hence the electron-optical magnification M is 3.75.

If the magnification is greater, the edges of the photo-emission image are projected outside the scanned area of the target. In other words, the scanned (and transmitted) image then corresponds to part of the photo-emission image only; the field is thus smaller and the effect is the same as if the camera were moved closer to the subject. It should be added, however, that the resolving power of the electron lens, even with the gauze, is so high that with $M = 3.75$ it by no means limits the definition of the image; as mentioned in article I, the definition is limited by the electron gun. Hence the image on the target remains sufficiently clear, even when the magnification is increased.

As stated in article I (p. 128), any reduction in the magnification below 3.75 results in an increase in the optical errors, e.g. curvature of field, until a point is reached when they can no longer be compensated. For this reason we shall in the following consider only a magnification of 3.75 or more.

In our discussion of fig. 3*a* we remarked upon the possibility in principle of varying the magnification by axially displacing the focusing coil; when it is moved away from the target (which corresponds to a reduction in the effective length of the magnetic field) the magnification is increased. However, most cameras provide little opportunity for displacement in this direction owing to the fact that a short-focus objective is used and that the coil would quickly come to rest against the lens mounting. Movement of the coil is therefore only resorted to in order to adjust the magnification to a particular value once and for all. At the same time, the effective length of the magnetic field can also be varied by electrical means [7]). Something in the shape of a focusing coil in two sections might be visualised *(fig. 6)*. If only that section which is at the photo-cathode end be energized, a short magnetic field will result and the magnification of the image will

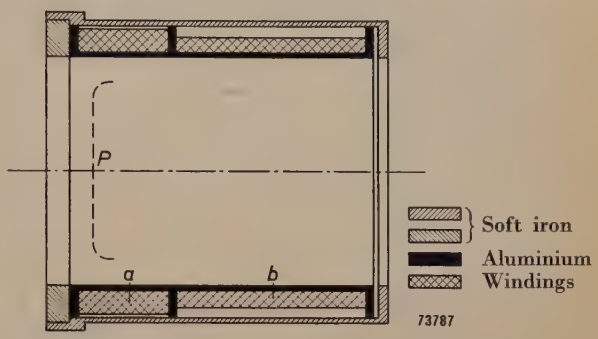

Fig. 6. Experimental focusing coil in two sections *a* and *b*, for continuous variation of the electron-optical magnification. P = relative position of the photo-cathode.

be higher than usual. With current applied to the other section, the current flowing in the first being simultaneously reduced to restore the focus, the image of the photo-cathode on the target will be smaller than before. The diagram in *fig. 7* shows the magnification M plotted against the current I_2 flowing in the second coil, as well as the current I_1 in the first coil required to maintain a sharp image. These measurements were obtained from an image iconoscope with

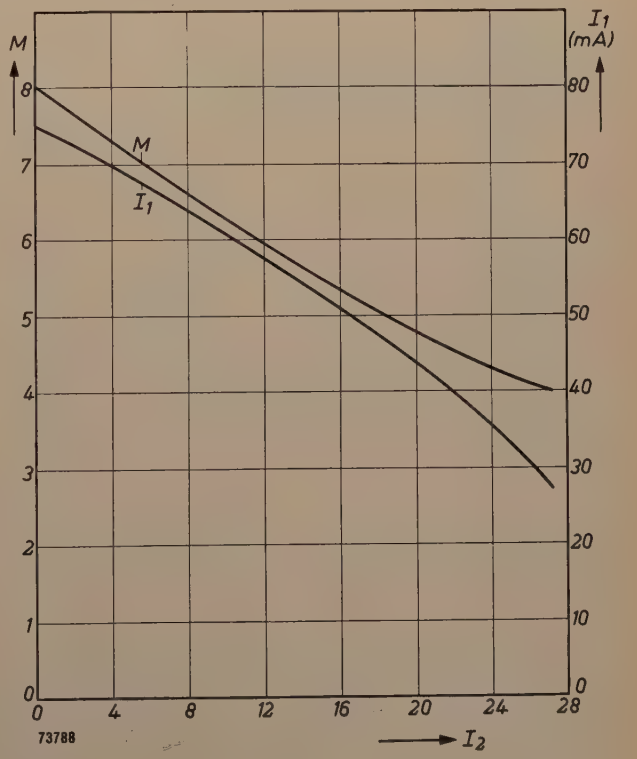

Fig. 7. The electron-optical magnification M as a function of the current I_2 flowing in section (*b*) of the coil shown in fig. 6. I_1 is the current that must flow in section (*a*) to ensure good definition.

[7]) J. C. Francken,, Tijdschrift Nederlands Radiogenootschap, **16**, 243-257, 1951 (No. 5), in particular p. 252-256 (in Dutch); H. Bruining, Le Vide **7**, 1248-1255, 1952 (No. 42) (in French).

gauze, in conjunction with the coil depicted in fig. 6. In this way, then, we have already achieved an appreciable variation in the magnification.

There is, however, a big disadvantage in this method. As outlined in article I, the electron-optical image is subject to a rotation of the potential pattern on the target with respect to the emission-image on the photo-cathode. It is found that when the magnification is varied in the manner just described, the angle of this rotation varies as well, which is most undesirable.

It would be possible to make some compensation for this rotation by turning the tube an equal amount in the opposite direction inside the camera, but, obviously, this would be a makeshift and complicated arrangement. By ascertaining the factors governing the angle of rotation it has been found possible to evolve a design in which the angle remains constant while the magnification is varied.

Relationship between magnification and angle of rotation

The following experiments have thrown more light on the dependence of the rotation of the image on the form of the magnetic field.

Use was made of the kind of focusing coil depicted in *fig. 8*. This consists of two sections enclosed in a

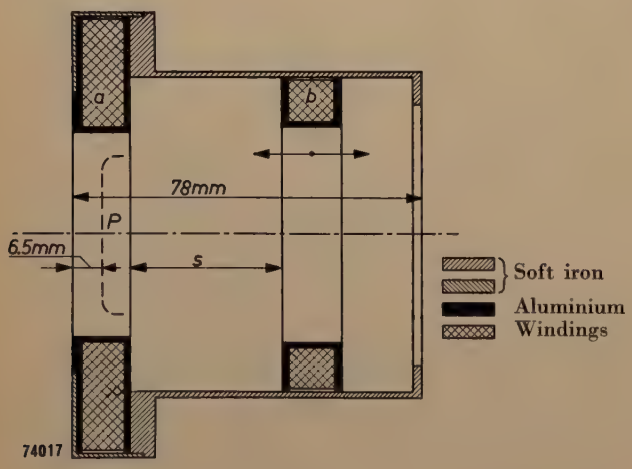

Fig. 8. Experimental focusing coil with fixed section (*a*) and adjustable section (*b*). P = relative position of the photo-cathode.

soft iron housing; the section facing the target is movable. The experiments were carried out on a tube which had been provided with a gauze. Very similar results were obtained, however, from a tube without a gauze.

The angle of rotation Ψ was determined as a function of the magnification M, for several different positions of the movable section of the coil. The results of some of the measurements are shown graphically in *fig. 9*. The parameter in this figure is the distance s between the two coil sections. With

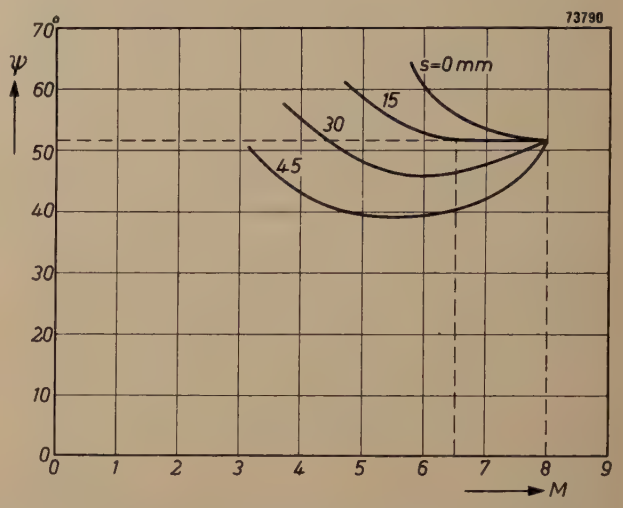

Fig. 9. The angle Ψ through which the image on the target is rotated with respect to the image on the photo-cathode, as a function of the electron-optical magnification M. The parameter varied here is the distance s between the two sections of the coil (fig. 8).

maximum magnification ($M = 8$) no current flows in coil section *b*, so that Ψ is then independent of s, that is, the curves meet at a common point.

The following conclusions may be drawn from the chart:

1) A particular magnification can be obtained with magnetic fields of different forms, but the angles of rotation then differ: the straight line $M =$ constant is intersected by the curves $\Psi = f(M)$ at various points, which means that the angles differ.
2) The slope of the curves in the region of $M = M_{max}$ is negative when the second coil section is close to the first, but becomes more and more positive according as it is moved in the direction of the target.
3) The angle of rotation has a minimum in those cases where the curves have positive slopes at $M = M_{max}$.

It follows from conclusion 2) that the angle of rotation in the vicinity of $M = M_{max}$ can be kept constant by finding the appropriate position of the second coil section (see curve for $s = 15$ mm). The magnification range extends only from $M = 8$ to $M = 6.5$. In order to ensure a constant angle between more widely separated limits of the magnification, the second coil section in fig. 8 has to be divided in two *(fig. 10)*; the two sections thus obtained must then be so adjusted that one of them

produces a positive slope of $\Psi = f(M)$ near $M = M_{max}$, and the other a negative slope, so that the two effects compensate each other. It has actually been found possible in this way to maintain a constant angle of rotation between wide limits of the magnification, and fig. 10 shows the arrangement for a coil which will allow of variation in the magnification in the ratio of 1 : 2, with constant angle of rotation.

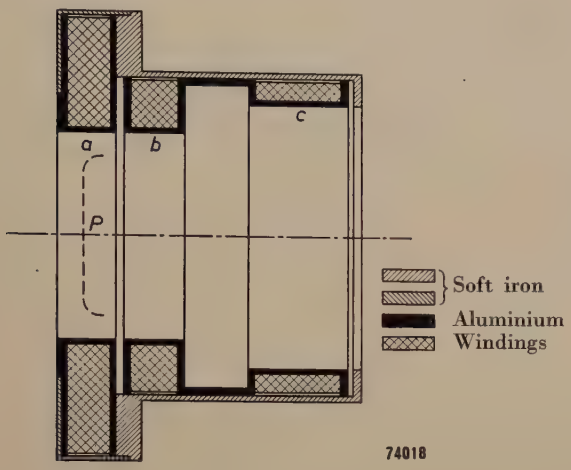

Fig. 10. Focusing coil with three fixed sections (*a*), (*b*) and (*c*) which can be separately energized. P = relative position of the photo-cathode.

Fig. 11 illustrates the current in the three coil sections plotted against the magnification. For continuous variation of the magnification these currents must be so adjusted, simultaneously, that the curves as shown in this figure are reproduced. The method employed to achieve this is described in the last section of this article.

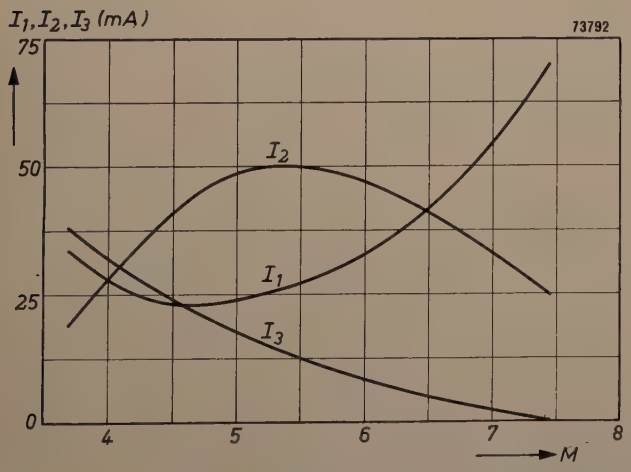

Fig. 11. The currents I_1, I_2 and I_3 which must flow in the three sections of the focusing coil (Fig. 10) to ensure high definition and almost constant angle of rotation Ψ plotted against the magnification M. M can be varied continuously in the ratio of 1 : 2.

The magnetic field of the focusing coil protrudes to a certain extent in the space within which the scanning beam moves. The beam cuts the magnetic lines of force almost at right angles and the extent to which the beam is consequently deflected is more marked at the top of the target than at the bottom, the scanned figure being accordingly a parallelogram instead of a rectangle (diamond distortion). This may be corrected by placing a small coil between the focusing coil and the target to compensate locally the field of the focusing coil. The current flowing in this small coil would have to be proportional to the current in the third section of the focusing coil, which contributes by far the most towards the field in the scanning space. The compensating coil, shunted by a resistor which would be adjustable and subsequently locked permanently, would accordingly be placed in series with the third coil section. In figs. 13 and 14 this is not shown.

We may add here that a coil in three sections (fig. 10) proved to be a very suitable basis for the design of a coil to give a fixed magnification (3.75 ×) in the image iconoscope fitted with gauze. By energizing the three sections in different ways we have been able to find the optimum image with the desired magnification and, from the values of the current in the three coil sections it was finally found possible to work out details for a single coil having different numbers of turns per centimetre in the axial direction. A sketch of such a coil is shown in *fig. 12*; the form of the resultant field is such that the image exhibits little or no distortion, and only traces of curvature.

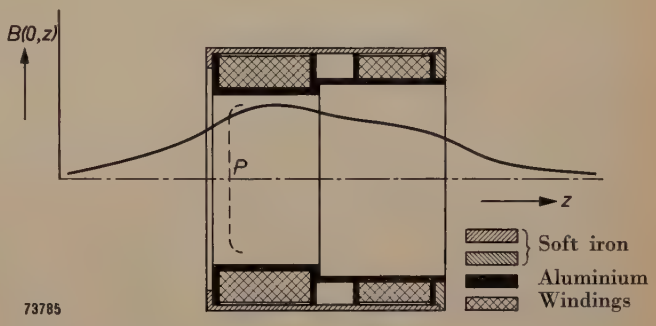

Fig. 12. Focusing coil with two sections in series to give constant magnification (M = 3.75) in the image iconoscope with gauze. P = relative position of the photo-cathode.

Practical application of the variable magnification

In order to incorporate the variable magnification described above in a T.V. camera, it is necessary to adjust the currents flowing in the three sections of the magnetic lens in accordance with the curves depicted in fig. 11. For this purpose each coil can be connected to a potentiometer (*fig. 13*). In practice it is essential that the three potentiometers be operated by a single control. For the first section an

ordinary linear potentiometer can be used; the two others should conform to special laws such that the values of this currents I_2 and I_3 will suit each value of I_1 in accordance with fig. 11.

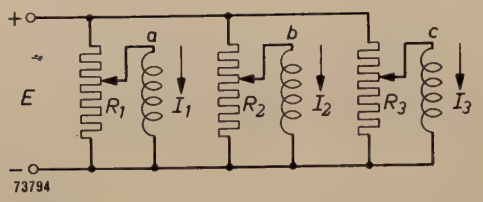

Fig. 13. Circuit for simultaneous control of the currents I_1, I_2 and I_3 in the three sections a, b and c of the focusing coil. E = constant control voltage. R_1, R_2, R_3 = variable potentiometers.

A drawback of this arrangement is that the resistance values of the coil sections, as well as those of the potentiometers, tend to vary with changes in temperature. For this reason it is better to connect a high-impedance electron tube in series with each coil. The grid bias of each of the three tubes can then be controlled so as to provide an anode current of the required value. A suitable circuit [8]) is shown in *fig. 14*.

For the purposes of fig. 13 it was tacitly understood that I_1, I_2 and I_3 were monotonically rising or falling functions of M but, in fact, as will be seen from fig. 11, only I_3 is a descending curve, whereas I_1 exhibits a minimum and I_2 a maximum. In order to be able to control these three currents in the desired manner with a single control knob we have, therefore, devised a special circuit for the potentiometers R_1 and R_2 (see fig. 14). R_1 has a fixed tapping connected to the negative line, the two extremities being taken to the positive; R_2 also has a fixed tapping, but this is connected to the positive line, with both ends of the track to H.T. negative. When the control knob operating R_1, R_2 and R_3 is so adjusted that the slider of R_1 coincides with the tapping point, tube P_1 receives maximum negative bias, i.e. I_1 is at its minimum. Rotation of the knob one way or the other causes I_1 to rise. When the adjustment is such that the slider of R_2 lies on the tapping point, tube P_2 receives minimum negative bias and I_2 is at a maximum.

Finally, a few remarks about the sensitivity of the camera tube when operated with variable magnification. It will be obvious that when a change is made from an effective area of the photocathode of 20 mm diagonal to another having a diagonal of only 10 mm, the average effective photo-current for that particular area will be smaller. The actual decrease will depend on the amount of information contained in the scene being televised, but, when the brightness of the scene is roughly uniform, the average photo-current will drop to 1/4 of its original value. From fig. 18 in article I it appears that the signal delivered by the tube does decrease. The result is a dimmer image.

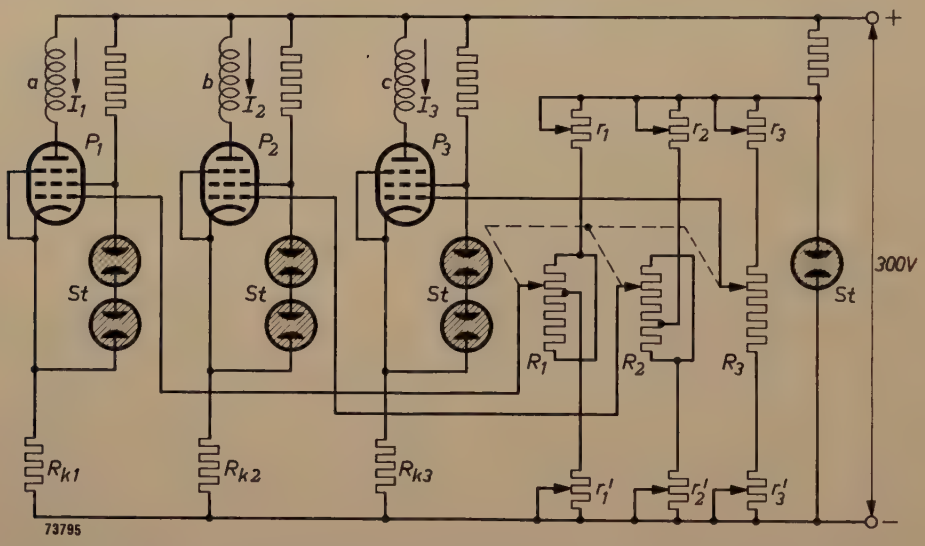

Fig. 14. Improved circuit for the simultaneous control of currents I_1, I_2 and I_3 in the three sections a, b and c of the focusing coil. P_1, P_2 and P_3 each denote two pentodes type PL 83 connected in parallel. St = stabiliser tubes type 85-A1. R_1, R_2, R_3 = potentiometers operated by a single control knob. r_1, r_2, r_3 and r_1', r_2' r_3' = correcting resistors. R_{k1}, R_{k2} and R_{k3} = biasing resistors producing strong negative feed-back so that the anode currents shall be independent of the valve characteristics.

There are two ways of maintaining a constant level of video signal. The first of these consists of ensuring by optical means that the illumination on the photocathode varies in inverse proportion to the effective area of the cathode. One way of doing this is to use larger stops as the effective area of the photo-

[8]) Designed by A. J. Sietsma of this laboratory.

cathode is reduced. The other method is based on electrical compensation, viz. an increase in the amplification factor of the video amplifier when the magnification of the camera tube is increased.

Clearly, neither of these two methods can be carried very far. In the first instance very fast lenses are used — even with a photo-cathode of 20 mm diameter — and only a limited use can be made of the stop; in the second instance too much amplification results in too much background noise. This means that with the camera tube type 5854/02 we are restricted, in the matter of variation of the magnification, to a factor of 2.

Another limitation on the use of very small areas of the photo-cathode is imposed by the resolving power of the lens, as will be clear when we compare the case of a photo-cathode of which full use is made, with one that is used only in part; in both cases the definition (the number of lines in the height of the image) must satisfy the same minimum requirement. The resolving power of the lens (number of lines per centimetre that can be resolved) has therefore to conform to the highest standard for the cathode when only part of this is used. In addition, the stop used in the latter instance has to be larger (see above).

On the basis of very recent experiments it has been found possible to design a soft iron housing for the coil, such that the maximum diameter of the effective part of the photo-cathode can be increased from 20 mm to 25 mm, enabling the magnification to be adjusted up to a ratio of 1 : 2.5 without the disadvantages mentioned above becoming apparent.

Summary. In image iconoscopes positive ions are produced which migrate towards the photo-cathode. In the older type of tube the non-uniform electric field concentrates these ions upon a small area of the photo-cathode with the result that this area rapidly loses sensitivity (ion burn or ion spot). In the new Philips image iconoscope (type 5854/02) a fine metal gauze is mounted at the end of the anode cylinder, facing the photo-cathode. Between this gauze and the cathode the electric field is uniform, the positive ions are accordingly distributed uniformly over the whole area of the photo-cathode and the occurrence of an ion spot is eliminated.

Provision of the gauze brings with it another advantage, namely a reduction in the (already small) amount of rotational distortion in the electron-optical image of the photo-cathode on the target. As against these advantages there is but one drawback, a slight reduction (20 to 25%) in the sensitivity, as a result of interception of electrons by the gauze.

A second improvement in the image iconoscope concerns the control on the field of view, which is now variable in size by wholly electrical means, necessitating no complicated optical systems. For this purpose the magnetic focusing coil is made in three sections, which are energized separately. The three currents can be controlled simultaneously, so that the electron-optical magnification, and with it the field of view, can be varied continuously in the ratio of 1 : 2. At the same time the image remains sharp and the angle through which the image is rotated with respect to that on the photo-cathode remains practically constant. A circuit is described which enables the energizing currents for the three sections of the focusing coil to be adjusted in the desired manner by means of a single control knob.

A RUBBER MEMBRANE MODEL FOR TRACING ELECTRON PATHS IN SPACE CHARGE FIELDS

by G. A. ALMA, G. DIEMER and H. GROENDIJK. 537.533.3.072:621.385.1

The rubber sheet has for some time been a well-known medium for the investigation of two-dimensional fields and the motion of electrons within them. It has been found possible in the development of electron tubes by this means to obtain a better insight into many problems, in particular in cases where purely theoretical treatment presents great difficulty. The method is also useful when applied to ultra-short-wave valves, where the electrode spacing is extremely small, provided that allowance be made on the rubber sheet for the space charge produced by the electrons themselves. A practical method of doing this, and the principles on which the method is based, are described in the following.

The motion of the electrons in electron tubes can be imitated by rolling steel balls over a surface which is a "model" of the electrostatic field in the valve; a stretched rubber sheet forms a conveniently deformable surface for the purpose. The vertical distance h of such a surface from a fixed horizontal surface is at every point (X,Y) proportional to the potential φ at the corresponding points (x,y) in the field. Furthermore, the horizontal projections of the tracks of the steel balls in the model are of the same form as those of the electrons in the electrostatic field; the velocities of the balls and electrons are also proportional. The proof of this may be found in an article by Kleijnen which appeared in this Review some time ago[1]) and which will be referred to in the following as I.

Fig. 1. The movement of electrons in an electrostatic field can be imitated by rolling steel balls over a stretched and appropriately supported rubber sheet. When photographed with intermittent light the tracks of the polished steel balls are seen as dotted lines. The velocity can be ascertained from the spacing of the dots.

The paths and velocities of the brightly polished steel balls are determined by photographing them with intermittent light of known periodicity; in this way these paths are rendered visible as dotted lines (*fig. 1*), the velocity being ascertained from the spacing of the dots.

Imitating the space charge by exerting pressure on the rubber sheet

In his work Kleijnen assumed that the electrostatic field did not include a space charge (see I, pp. 338-339), but we shall extend our considerations to make allowance for a space charge. We proceed from the assumption that the rubber sheet is first stretched with a constant tension σ in a horizontal plane XY. We then consider the situation when the sheet is displaced vertically; the vertical deflection h of any point will be a function of its coordinates X and Y and, in the general case, also of the time t. It is assumed, further, that a vertical pressure p operates on the sheet, which in general will also be dependent on X, Y and t. The tension of the sheet (see I) results in a vertical force on an element of dimensions $\mathrm{d}X$ and $\mathrm{d}Y$ equal to:

$$\sigma\left(\frac{\partial^2 h}{\partial X^2}+\frac{\partial^2 h}{\partial Y^2}\right)\mathrm{d}X\,\mathrm{d}Y.$$

The pressure results in a vertical force $p\ \mathrm{d}X\ \mathrm{d}Y$. Let m_1 denote the mass per unit area; the equation of motion will then be:

$$\sigma\left(\frac{\partial^2 h}{\partial X^2}+\frac{\partial^2 h}{\partial Y^2}\right)+p=m_1\frac{\partial^2 h}{\partial t^2}. \quad . \ . \ . \quad (1)$$

[1]) P. H. J. A. Kleijnen, The motion of an electron in two-dimensional electrostatic fields, Philips tech. Rev. **2**, 338-345, 1937, in particular page 340. The method can be employed only when the field is independent of one of the three mutually perpendicular coordinates.

We are interested only in the case where the rubber sheet is in equilibrium [2]); then $\partial^2 h/\partial t^2 = 0$ and p is independent of time, so that equation (1) is reduced to:

$$\frac{\partial^2 h}{\partial X^2} + \frac{\partial^2 h}{\partial Y^2} = -\frac{p}{\sigma} \quad . \quad . \quad . \quad . \quad (2)$$

This is Poisson's equation, which is also valid for the potential φ in electrostatic fields with space charge. If the density of the space charge be denoted by ϱ, we may write for this potential in a two-dimensional field (co-ordinates x and y):

$$\frac{\partial^2 \varphi}{\partial x^2} + \frac{\partial^2 \varphi}{\partial y^2} = -\frac{\varrho}{\varepsilon_0} \quad . \quad . \quad . \quad . \quad . \quad (3)$$

where $\varepsilon_0 = 8.855 \times 10^{-12}$ A.sec/V.m, the dielectric constant of free space.

The rubber membrane is prepared in such a way that the following relationships exist between the co-ordinates of corresponding points in the field and model:

$$\left.\begin{aligned} x &= S_l X \\ y &= S_l Y \end{aligned}\right\}, \quad . \quad . \quad . \quad . \quad . \quad . \quad . \quad (4)$$

where S_l is a scale factor for the length dimension. It is also required that the vertical displacement of the rubber sheet and the potential of the field at corresponding points are related as:

$$\varphi = S_\varphi h. \quad . \quad . \quad . \quad . \quad . \quad . \quad . \quad (5)$$

where S_φ is the scale factor for the potential.

By applying (4) and (5) to (3) and then comparing this differential equation with (2), we find that p should conform to:

$$p = \frac{S_l^2}{S_\varphi} \frac{\sigma}{\varepsilon_0} \varrho. \quad . \quad . \quad . \quad . \quad . \quad . \quad (6)$$

The solution of Poisson's equation (2) or (3) is uniquely determined if the right-hand term is given as a function of the co-ordinates and provided that the boundary conditions are known. In this case the boundary conditions are that the potentials at the surfaces of the electrodes should have specified values. In order to obtain the desired model of the field, therefore, we must apply a pressure at every point on the rubber sheet that will be in accordance with (6); the mechanism employed to ensure this is described at a later stage. Moreover, we must produce deflections h along the lines corresponding to the edges of the electrodes, that will be related to the potentials of these electrodes in accordance with (5).

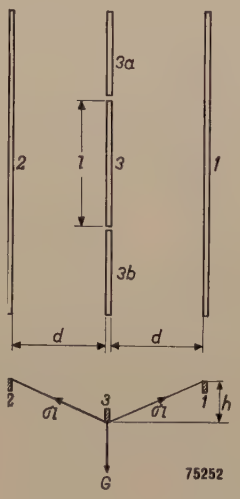

Fig. 2. Method of determining the tension in the rubber sheet. The parallel rods *1* and *2* are mounted horizontally and the rubber sheet is laid over them. Rod *3* (length l) is depressed with a known force G; the sag h resulting from this force is then measured. The additional rods *3a* and *3b*, which are pressed down to the same depth as rod *3*, serve to counteract the effect of the finite length of rod *3*. From the lower figure, which is also the diagram of forces, it is found that when $h \ll d$, $G = 2\,\sigma l h/d$, from which it follows that $\sigma = Gd/2lh$.

To be in a position to employ equation (6) we must apparently know the tension σ of the sheet; this is determined experimentally by measurement in the manner shown in *fig. 2* and described in the caption to the figure.

Method of successive approximation

As will be apparent from the foregoing, the space charge distribution must be known in order that the model can be made.

Apart from the number of electrons, however, the space charge depends on their paths and velocities, which are just those unknowns that have to be determined from the model. A way out of this difficulty is offered by the method of successive approximation. A model is first made without space charge (pressure), or still better, with a pressure corresponding to a plausible space charge distribution; from the motion of the steel balls then observed, the corresponding density of the space charge can be computed [3]) and the distribution

[2]) In the absence of equilibrium and assuming $p = 0$ (which means that there is no pressure on the rubber sheet), equation (1) takes the form:

$$\frac{\partial^2 h}{\partial X^2} + \frac{\partial^2 h}{\partial Y^2} = \frac{m_1}{\sigma} \frac{\partial^2 h}{\partial t^2}.$$

This is known as the wave equation, and describes transverse vibrations of the rubber sheet. These vibrations are analogous to the electromagnetic waves occurring in cavity resonators. This analogy has been used in this laboratory in a study of the performance of cavity resonators; see K. S. Knol and G. Diemer. Philips tech. Rev. **11**. 156-163, 1949.

[3]) The contribution of an electron to the average space charge in a given volume element is proportional to the time that the electron dwells in this element. This time is in turn proportional to the number of dots produced on the photograph by the steel ball when traversing the corresponding surface element of the rubber sheet. Intuitively it may be said that the density of the space charge can be derived from that of the dots in the photograph, but further discussion of this point would take us beyond the scope of the present article.

of pressure modified accordingly. The steel balls are then again rolled over the sheet, the space charge distribution being again computed, and so on.

In general this procedure may be expected to yield an increasingly closer approximation to the correct solution, and a number of simple examples in which the method of successive approximation can be verified mathematically have shown that this can, in fact, be achieved quite quickly. Nevertheless, in certain instances the convergence may prove to be too slow, or there may actually be divergence (see Appendix).

Some experiments, which are described in the following, confirm the assumption that rapid convergence usually does take place [4]).

Experimental equipment

Charged particles are repulsed by a space charge of their own polarity. When they enter a zone in which such a space charge exists, their potential, therefore, is greater than in the absence of the space charge; hence, in the model, an upward pressure on the rubber sheet will correspond to a space charge. This upward thrust is provided by a number of pads to which a vertical force is applied, the amount of force per pad being variable. The forces are supplied by weights and are applied by means of wires and pulleys. A number of units (each having six such pressure pads, *fig. 3*) can be used at a time, this being a very convenient method, capable of representing a wide range of electrode configurations.

To minimize possible irregularities in the surface of the rubber sheet at the points where the boundaries of the pressure pads occur, the latter are made of sponge rubber and are mounted in such a way that they will tilt easily.

It is essential that the forces as adjusted shall operate regardless of the height ultimately assumed by the rubber sheet, and the unit described fulfils this condition. Pressure applied by means of electromagnets, a method which was tried and which has the advantage of simple remote control, does not sufficiently meet this requirement.

Owing to friction in the apparatus, the forces applied to the sheet are not strictly in accordance with the loading weights. It is possible to introduce a correction for this, but friction should in any case be kept to a minimum. In the unit shown in Fig. 3, the friction is less than 5% of the weight applied. For some of the experiments use was made of another, less efficient mechanism, in which friction accounted for 15% of the applied weight. Reference to the method of compensating the friction losses will be made later.

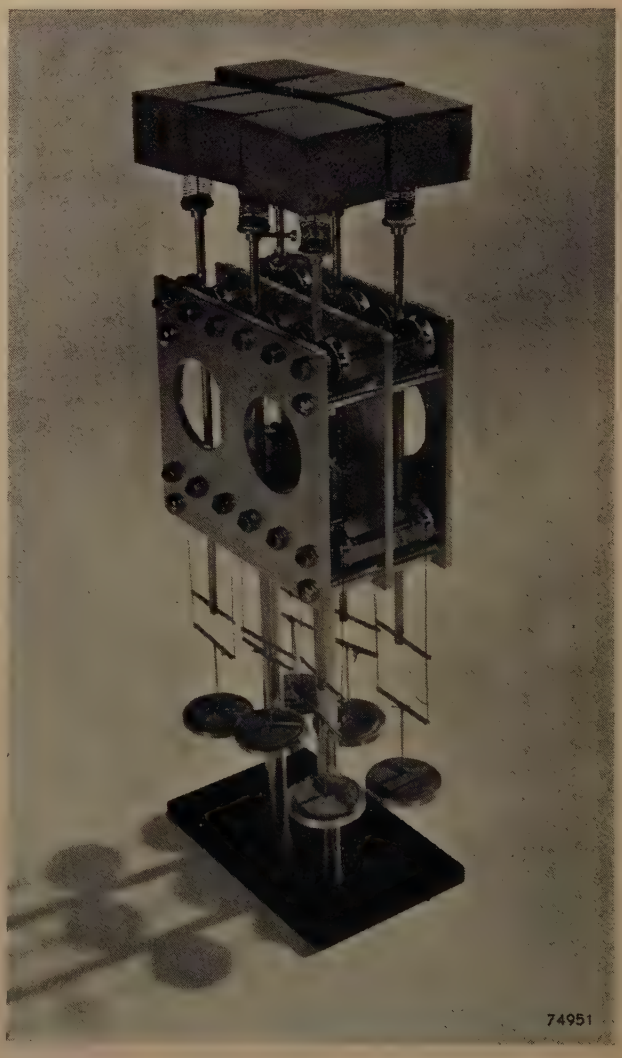

Fig. 3. Unit for applying upward pressure to the rubber sheet. This pressure represents the space charge produced by the electrons. A number of such units placed side by side can be used to imitate any distribution of space charge. The dimensions of the pressure pads are 3 cm x 3 cm.

[4]) Mention has already been made in I of the method of successive approximation as a possible means of taking into account the space charge caused by the electrons themselves. It is however only when this process is used in conjunction with the method of imitating the space charge by applying pressure to the rubber sheet that the process can be used successfully for practical purposes. In principle, it is possible by applying a numerical solution of Poisson's equation, to compute the correction that has to be made in the depth of the rubber sheet to allow for the space charge, but this entails an enormous amount of work. Moreover, after the first stage, the rubber sheet would have to be replaced by a series of rigid computed surfaces which, of course, would be impracticable. The idea of representing the space charge by a variable pressure has in the meantime also been suggested by Bloch in a discussion subsequent to a lecture on the errors in the rubber sheet (Proc. Inst. El. Engrs. **97**, II, 443, 1950, and also independently by the Russian scientists Bobykin, Kelman and Kaminsky, who have made practical use of this method (J. tech. Phys. USSR, **22**, 736-743, 1952). They employed apparatus very similar to ours (and also applied the pressure by means of plates loaded with weights).

Experiments to test the method

In order to test the method three sets of conditions were imitated on the rubber sheet, relating to configurations in which the electron paths were already known; tests carried out with the rubber sheet yielded these results with a very reasonable degree of accuracy, thus considerably adding to our confidence in the method.

Rubber sheet shaped cylindrically

The first experiment described was intended to examine the effect of the separate pressure pads on the paths of the steel balls: it was feared that irregularities might appear in the surface of the sheet at the transitions between adjacent pads. Such discrepancies would have represented a departure from the theoretical paths and, especially with low velocities, this might be quite pronounced.

The apparatus used for this test is depicted diagrammatically in *fig. 4a*. The rubber sheet was curved in one direction only, namely the X-direction the trough being obtained by placing the sheet on a metal box, the hollowed top of which was perforated, so that, with the box connected to a vacuum service line, the sheet would be firmly held in position. Further along, the sheet was restored to the horizontal by a smooth, cylindrically curved plate of radius R. This plate was made in three pieces, as shown by the dotted lines in fig. 4*a*, the dimensions being such that, with the centre part removed, there would be just enough room for a pressure unit with six plates.

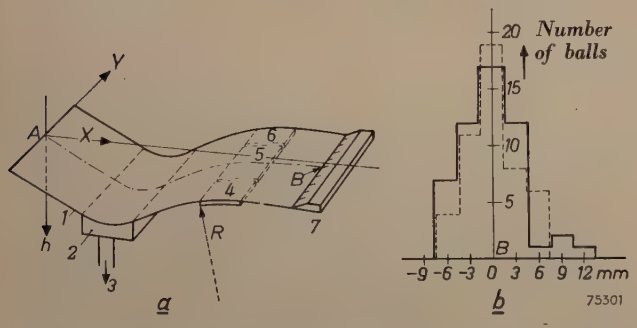

Fig. 4. *a*) Diagram illustrating the method employed for checking the effect of the arrangement of pressure pads in the space charge unit (fig. 3) upon the tracks of the steel balls. *1* rubber sheet, *2* box with perforated upper surface, connected to vacuum pump *3*; *4*, *5* and *6* cylindrical metal plates imparting to the rubber sheet a curvature of radius R. Plate *5* can be replaced by the space charge unit shown in fig. 3. *7* rule.
b) Deviation from the point B, of the points of arrival of steel balls started at A. The ordinate indicates the number of balls arriving within the distance shown by the abscissa. The full line refers to the rubber sheet as supported by the metal plate *5*, and the broken line to the case where the plate is replaced by the space charge unit.

Under these conditions the theoretical values are easily calculated for the forces with which the pressure plates should be loaded in order to reproduce as faithfully as possible the contour of the smooth metal plate. It was found that the necessary pressure on the whole of the supported surface must be constant at $p = \sigma/R$. A check was made to see whether these computed loads would yield the desired contour without serious irregularities, and for this purpose steel balls were started from the point A (Fig. 4*a*), without initial velocity; in the ideal case these should all have arrived at the point B, lying opposite to point A in a direction perpendicular to the "electrodes". In actual fact, with both the smooth plate and the "space charge apparatus", a certain amount of spread occurred at the point of arrival, and this was measured by means of a rule placed at B. The number of balls arriving within certain limits is shown in the chart in Fig. 4*b*. Although the velocity at and after passing the supporting plate of radius R was low, so that the effect of irregularities in the surface of the rubber sheet might well have been quite pronounced, the diagram shows that the deviations were very similar in both cases. Apparently, then, differences caused by imperfections in the space charge model are only slight compared with those due to other causes.

Pierce electron gun

As an instance intended to demonstrate the speed with which the method of successive approximations yields results, a form of the well-known Pierce electron gun [5]) was reconstructed. In this type of electron gun the form of the electrodes is such that the electrons travel from the cathode to the anode in a parallel beam, despite their natural repulsion (*fig. 5*). When no pressure was applied to the rubber

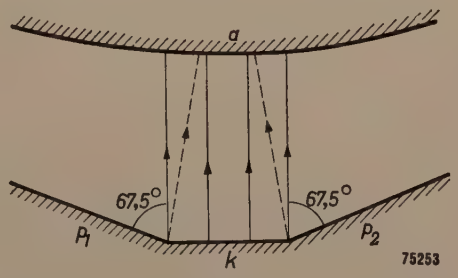

Fig. 5. Electrode configuration of the Pierce electron gun. k cathode; p_1 and p_2 auxiliary electrodes at cathode potential; a anode. On the rubber sheet the "electron paths" were within the broken lines, when no space charge (i.e. distributed pressure) was applied. With the "space charge" as derived from these paths the tracks at once became parallel.

[5]) J. R. Pierce, Rectilinear electron flow in beams, J. appl. Phys. **11**, 548-554, 1940; see also Philips tech. Rev. **13**, 216, 1952.

sheet (i.e. without space charge), the beam was found to converge to such an extent that, on arrival at the anode, it had roughly only half its original cross-section. When the density of the space charge was computed as a first approximation from the tracks obtained, pressure being then applied to simulate the corresponding distribution, the beam proved to be parallel within the limits of accuracy obtainable with the rubber sheet [6]).

This result was obtained in spite of the fact that the first approximation of the space charge distribution differed considerably from the actual distribution, which was known from Pierce's calculations [5]). A second approximation of the space charge could have been computed on the basis of the parallel beam obtained from the first approximation, and this would have been very close indeed to the actual conditions.

This example shows that the distribution of pressure as applied to the rubber sheet may deviate considerably from the true value, but that for practical purposes the balls nevertheless simulate very closely the actual electron paths.

Diode with thermal velocity distribution of the electrons

The case of the plane diode can be treated theoretically even if account is to be taken of the different initial velocities with which electrons are emitted from the cathode (thermal velocity distribution). In a plane diode, velocity components parallel to the electrodes have no effect on the transit time of the electrons, or on the distribution of the space charge and potential. In principle, therefore, we need not make any allowance for the directional distribution of the initial velocities. Nevertheless this has been done, with a view to the intended investigation of a triode in which the problem is now two-dimensional owing to the presence of the grid wires; here the influence of the directional distribution of the electrons becomes important.

The thermal distribution of the velocity in the direction perpendicular to the cathode is depicted in *fig. 6*. As it is obviously impossible to reproduce such a continuous distribution of velocities on the rubber sheet, this was approximated by a distribution in four velocity groups of equal intensity, that is with the same number of electrons in each group. In fig. 6 this division is represented by four zones of equal area, I to IV, in the space below the curve. Each group was imitated on the rubber sheet by five steel balls, started from the cathode normally and at angles of 30° and 60° from either side of the normal, all with the normal velocity component appropriate to the group [7]). The dependence of the emission on its direction,

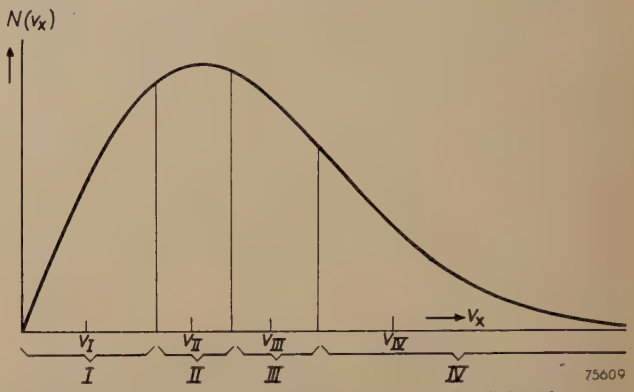

Fig. 6. Distribution of the forward velocity V_x of the electrons emitted by a heated cathode. The distribution is approximated to by division into four velocity groups, $V_I \ldots V_{IV}$.

which is known [8]), was taken into account in determining the space charge distribution from the dotted tracks in the photographs, by multiplying the dot density by the appropriate factors. To smooth out irregularities in the rubber sheet and so secure a better average, the experiment was repeated for different starting points at the

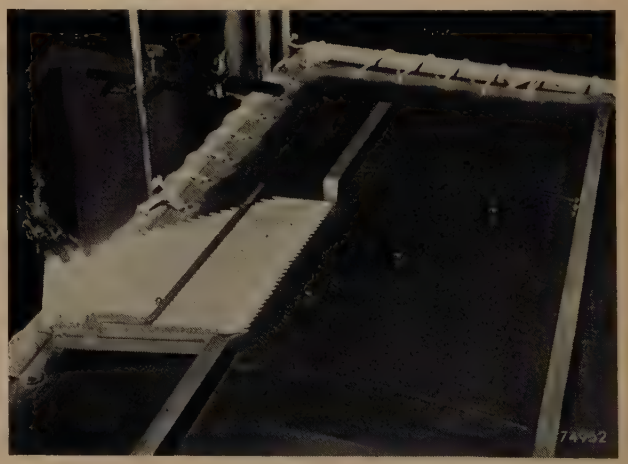

Fig. 7. View of the rubber sheet used for imitating the potential field of a diode. Two chalk lines have been made on the rubber sheet to demonstrate the curvature. At the left will be seen the starting chute used for imparting to the steel balls their initial velocity. In all the tests carried out, the balls were launched with sufficiently long intervals to prevent collision and too much indentation of the rubber sheet due to their combined weight.

[6]) Bobykin carried out the same check on the method, with the same results.

[7]) The arithmetic mean velocity of the electrons in a velocity group must not be used in this case. The contribution of an electron to a space charge in a volume element is proportional to the period that the electron dwells in the volume element, i.e. to the reciprocal of the velocity. For each group, therefore, the "appropriate" mean velocity is such that its reciprocal is the mean of the reciprocals for the electrons in that group.

[8]) See amongst others, W. G. Dow. Fundamentals of Engineering Electronics, Chapman and Hall, London, 1937, Ch. XI.

cathode. *Fig. 7* is a photograph of the rubber sheet used for reproducing the potential curve of the diode.

In this model a check was made to ensure that the sheet would assume the correct shape when pressure was applied in accordance with the exact space charge as computed from (6). The form of the sheet is depicted in *fig. 8*. The upper curve was obtained

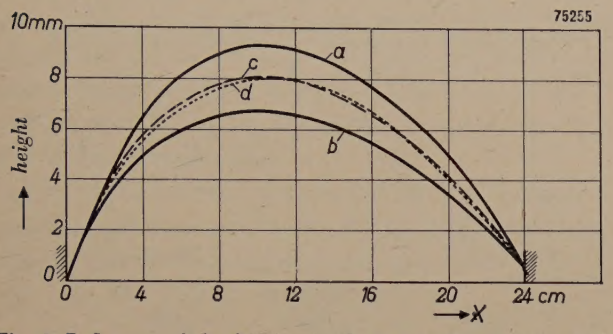

Fig. 8. Influence of the friction in the space charge unit which was the forerunner of the one depicted in fig. 3. The potential curve of a diode was imitated on the rubber sheet (see fig. 7). In the diagram the height of the sheet in the cross-section perpendicular to the electrodes is plotted. Curves *a* and *b* represent the extreme positions of the rubber sheet that it would assume as a result of the friction. Curve *c*, the mean curve of *a* and *b*, almost coincides with the theoretical curve *d*.

after the sheet had been allowed to settle slowly on the pressure pads, the lower after pushing the sheet down further than necessary and allowing it to rise. The mean of the two contours so obtained corresponds closely to the theoretical potential distribution. From the deviations shown by the extreme curvature compared with the average, it is seen that the friction in the space-charge apparatus represents a certain percentage (in this case 15%) of the load. In our experiments the rubber sheet was each time lowered very carefully on the pressure pads, so that all frictional forces were directed upwards, and a correction was made for these forces by making the load on the plates 15% less than the value provided by equation (6).

With the rubber sheet thus correctly shaped the steel balls were rolled with the above mentioned velocities and directions, and the space charge distribution was again computed from the paths so obtained. This should have agreed with the theoretical distribution taken as the starting point and, in fact, this was found to be very nearly the case (*fig. 9*). The difference between the true curve (*a*) and that obtained (*b*) may be attributed to the method employed in compensating the friction of the balls on the sheet [9]), namely by increasing their initial velocity. This is increased by an amount such that the correct velocity would be attained at the potential minimum; the electrons passing to the anode accordingly move too rapidly before reaching the potential minimum and, in that region, contribute too little towards the density of the space charge. Beyond the minimum they move too slowly and contribute too much.

Curves *c* and *d* in fig. 9 give some idea of the rate of convergence. A start was made on the basis of a space charge density corresponding to curve *c*, which at every point was twice the theoretical value and therefore incorrect. By rolling the balls and deducing the space charge distribution from the result, curve *d* was obtained, the average of which differs by less than 10% from the final result (curve *b*). When a start was made with a space charge equal to only one half of the theoretical value, the results also converged reasonably quickly (curves *e* and *f*). In both cases the error in the region of the potential minimum was quite small, even after the first stage of the process. *Fig. 10* shows the track of the balls as drawn from a photograph taken with intermittent lighting. These tracks refer to electrons starting at right angles to the cathode at three different velocities.

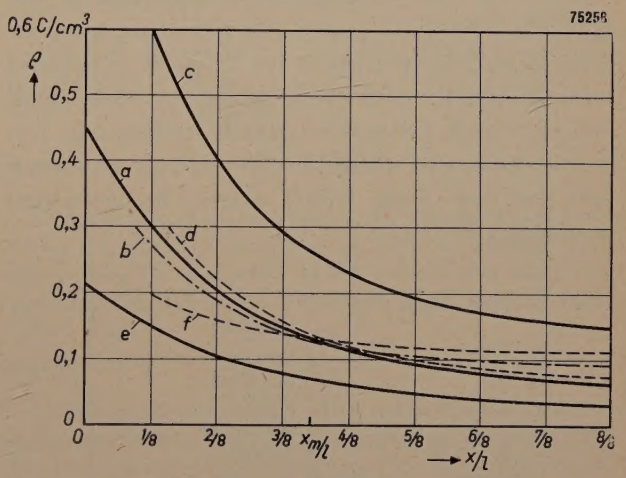

Fig. 9. Space charge density in a diode, as a function of the position co-ordinate x/l (l is the distance from cathode to anode). x_m/l represents the position of the potentional minimum.

Curve *a*. Theoretical distribution of the space charge.

Curve *b*. Derived from tests on the rubber sheet with pressure applied corresponding to the theoretical space charge distribution.

Curves *c* and *e* represent distributions with the space charge at all points twice, and one-half of the theoretical values respectively. Curves *d* and *f* were derived experimentally on the rubber sheet with a pressure corresponding to the space charge distribution of *c* and *e* respectively. Curves *c*, *d* and *e*, *f* give an idea of the rate of convergence of the method of successive approximation.

[9]) This friction should not be confused with that which is inherent in the space charge apparatus, to which reference has been made.

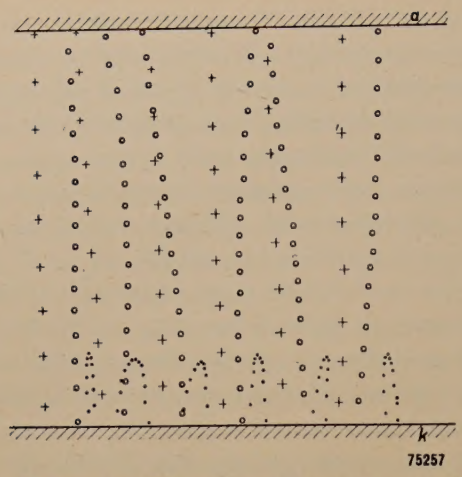

Fig. 10. "Electron paths" on the rubber sheet with which the potential field in a diode was imitated. The dotted tracks were drawn from photographs taken with intermittent lighting. Three different velocities were employed perpendicular to the cathode, these being represented by different symbols, viz. 0.84 v_m (•), 1.19 v_m (○) and 1.69 v_m (+); (v_m is the initial velocity at which the steel balls just reached the potential minimum). The deviation from the straight line must be attributed to irregularities in the surface of the rubber sheet.

Application to a micro-wave triode

After the tests described above the method was applied to the development of a new valve, a micro-wave triode. In such valves the diameter of the grid wire, although small (5μ), is not so very small compared with the grid-to-cathode spacing (*fig. 11*), in consequence of which the space charge assumes a very tortuous form which cannot be computed accurately.

We proceeded from a more or less plausible distribution of the space charge, computed by assuming the triode divided into sections, parallel to the grid wires and perpendicular to the cathode. These sections were regarded as ideal triodes, lateral deflection being disregarded. The method of computation has been described by Bennett and Peterson [10]) amongst others. A number of typical paths

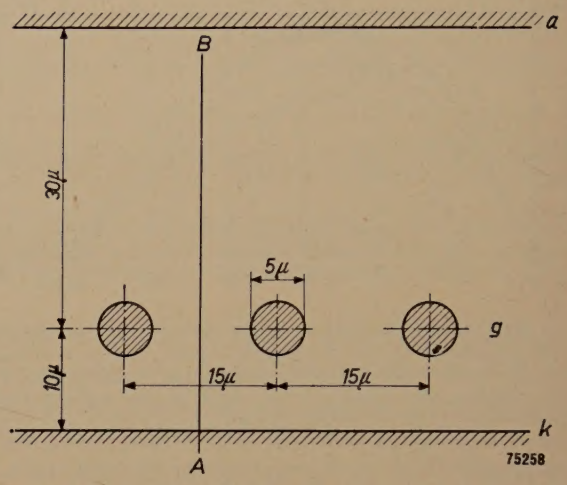

Fig. 11. Electrode configuration in a micro-wave triode. *k* cathode, *g* grid, *a* anode.

in the potential field produced by such a space charge are depicted in *fig. 12*. The "grid bias" employed corresponds to a high current density,

[10]) W. R. Bennett and L. C. Peterson, Bell Syst. tech. J. **28**, 303-314, 1949.

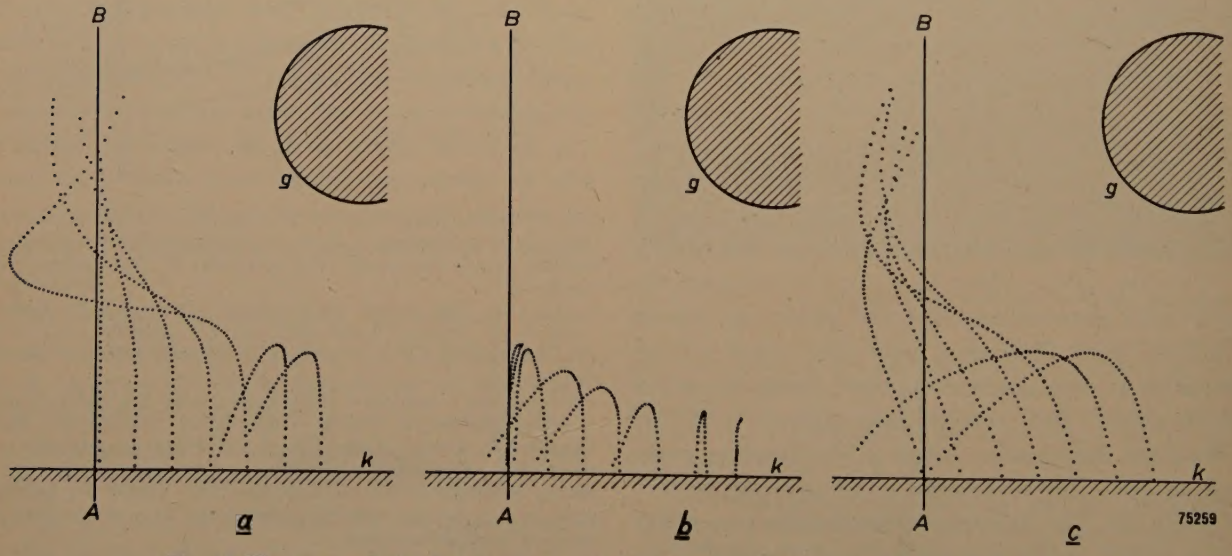

Fig. 12. Electron paths in a micro-wave triode as determined on the rubber sheet. The lines *AB* indicate the centre between two grid wires (cf. fig. 11).
a) Paths resulting from initial velocity perpendicular to the cathode: electrons passing the grid.
b) Paths resulting from a lower initial velocity, perpendicular to the cathode: electrons turned back by the grid.
c) Paths resulting from the same initial velocity as in (*a*), but started at an angle of 20° from the normal to the cathode.

although sufficiently below saturation to ensure only a low grid current.

The fact that so many electrons are deflected, and to such an extent, by lateral fields, shows that the distribution in the individual sections of the triode cannot be expected to give a fair approximation of the space charge in the entire triode. But, in view of the rapid convergence exhibited in the two preceding examples, it can be said with reasonable certainty that the photographed paths should not be far from the true paths, and that the space charge density computed from the paths as photographed should not differ very greatly from the actual distribution.

The pronounced differences in transit times (number of dots per track) of the electrons should also be noted. This is the reason for the drop in the slope in the higher frequencies.

Appendix: Convergence of the method of successive approximation

In the following we shall give two simple mathematical examples to demonstrate the rate at which the successive approximation process converges.

Both these examples relate to a static, uni-dimensional situation whereby all the electrons move in the positive x direction with the same initial velocity. The zero level of the potential φ is taken such that $\varphi = 0$ when the velocity of the electrons $v = 0$. The electron current, of density j, then gives the space charge density ϱ:

$$\varrho = \frac{j}{v} = j \sqrt{\frac{m}{2e}}\, \varphi^{-1/2}, \quad \ldots\ldots \quad (7)$$

where m = mass and e = charge of the electron.
Poisson's equation (3) assumes the form:

$$\frac{d^2\varphi}{dx^2} = -\frac{\varrho}{\varepsilon_0} \ldots\ldots\ldots\ldots \quad (8)$$

Mathematically, the successive approximation process comes to this, that in (8) we substitute for ϱ an arbitrary (simple) function $\varrho_0(x)$; the solution $\varphi_0(x)$ of (8) is then substituted in (7) and the function $\varrho_1(x)$ thus obtained is once more substituted in (8), the new solution $\varphi_1(x)$ again in (7), and so on.

For the solution of the differential equation (8) the integration constants are each time determined by the given electrode potentials.

In both examples we have also made a direct computation of φ (x). By substitution of (7) in (8) a differential equation for φ is obtained which is capable of solution [11]); the limit to which the approximation method should converge is therefore already known.

The plane diode

The first example refers to a plane diode. We will assume that the electrons leave the cathode ($x = 0$) without initial velocity and that the current is limited by the space charge.

[11]) See for example H. Rothe and W. Kleen; Grundlagen und Kennlinien der Elektronenröhren, Akad. Verlagsges. Leipzig 1943, p. 40. The solution as applied to the case of the plane diode is given on p. 20.

In this case the current density is found from the well-known Child's law (l = anode-cathode distance, φ_a = anode potential):

$$j = -\frac{4}{9}\varepsilon_0 \sqrt{\frac{2e}{m}} \cdot \frac{\varphi_a^{3/2}}{l^2} \ldots\ldots \quad (9)$$

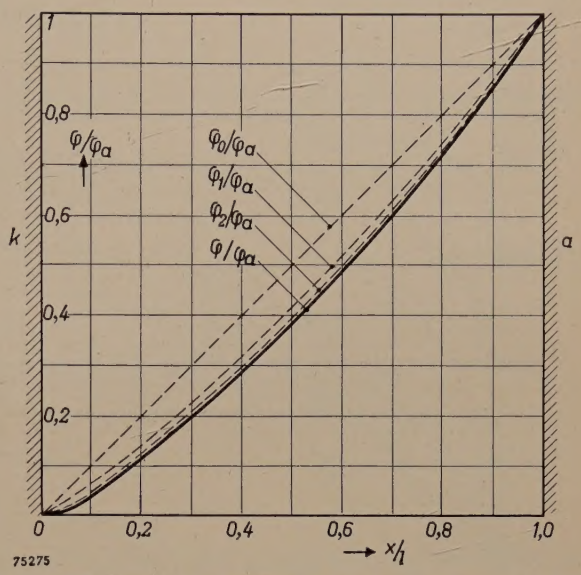

Fig. 13. The method of successive approximation applied to the potential distribution in a plane diode in which the current is limited by the space charge.

With this value of j, together with the boundary conditions $\varphi = 0$ when $x = 0$, and $\varphi = \varphi_a$ when $x = l$, the direct solution of (8) yields Langmuir's law:

$$\frac{\varphi}{\varphi_a} = \left(\frac{x}{l}\right)^{4/3} \ldots\ldots\ldots \quad (10)$$

This potential curve is shown in *fig. 13*, together with the successive approximations φ_0, φ_1 and φ_2 obtained with $\varrho_0(x) = 0$ as starting point. It will be seen that the second approximation is already almost the exact potential distribution (10).

Tetrode

The second example refers to the space between the screen grid g_2 and the anode of a tetrode, both being assumed to be at the same potential φ_a. The current density j is dependent on the control grid. Direct solution of $\varphi(x)$ is again possible, and yields the potential distribution plotted in *fig. 14* which, as

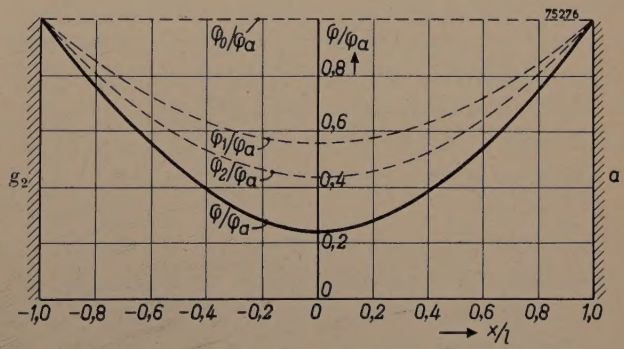

Fig. 14. The method of successive approximation applied to the potential distribution in the space between screen grid g_2 and anode a of a tetrode in which these electrodes are at the same potentional φ_a and in which the current density is maximum ($j/j_{max} = 1$). l = half distance g_2-a.

might be anticipated, reveals a minimum φ_m in the centre of the space between the electrodes. The depth of this potential minimum increases with j. Moreover, it is found that j cannot be increased beyond a certain maximum [12]), j_{max}, where $\varphi_m/\varphi_a = \frac{1}{4}$. j/j_{max} is employed as parameter, and the curve in fig. 14 is valid for $j/j_{max} = 1$.

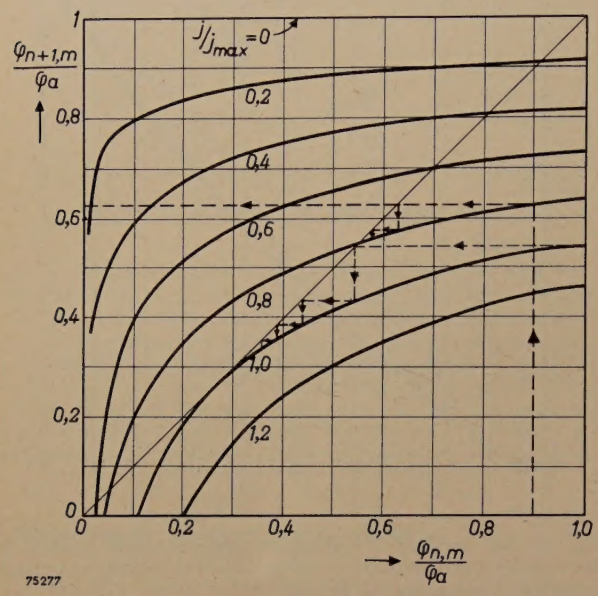

Fig. 15. Graphical representation of the process involved in the method of successive approximation as applied to a tetrode for different values of j/j_{max}.

Apart from the exact solution $\varphi(x)$, fig. 14 includes the successive approximations for φ_0, φ_1 and φ_2 obtained by starting from $\varrho_0(x) = 0$. It is seen that the second approximation $\varphi_2(x)$ still differs considerably from the true potential distribution. The function $\varphi_1(x)$, as will be seen from a simple calculation, represents a parabola. The function $\varphi_2(x)$ is so complex that the necessary integration to yield $\varphi_3(x)$ is too difficult to perform; nevertheless, with some sacrifice of accuracy we can proceed, for $\varphi_2(x)$ can be replaced as a close approximation by a parabola having the same minimum $\varphi_{2,m}$. Making use of this parabola we can then obtain $\varphi_3(x)$ and repeat the process. By means of an arbitrary parabola $\varphi_n(x)$ with a minimum $\varphi_{n,m}$, the minimum of the next approximation $\varphi_{n+1,m}$ can be computed as a function of $\varphi_{n,m}$, and this is illustrated in *fig. 15*, for various values of j/j_{max}.

If we assume for example that $j/j_{max} = 0.8$ and that $\varphi_{0,m}/\varphi_a = 0.9$, we find from the curve for $j/j_{max} = 0.8$ a value of 0.63 for $\varphi_{1,m}/\varphi_a$; this is used as starting point on the abscissa to evaluate $\varphi_{2,m}/\varphi_a$ and so on.

The stepped line between the curve for the selected value of j/j_{max} and the straight line $\varphi_{n+1,m} = \varphi_{n,m}$ demonstrates the rate at which the final result is approached.

The approximation $\varphi_0(x)$ obtained when using $\varrho_0(x) = 0$ as starting point, i.e. the horizontal line in fig. 14, can also be regarded as a parabola with a minimum $\varphi_{0,m} = \varphi_a$. If a start be made with zero space charge, the stepped line in fig. 15 must commence at $\varphi_{0,m}/\varphi_a = 1$.

It will be seen that the convergence is reduced according as j/j_{max} is moved towards unity; if we take $j/j_{max} > 1$, the method of successive approximation is no longer convergent, as already mentioned in footnote [12]).

Summary. The motion of electrons in two-dimensional electric fields can be imitated by rolling steel balls over a surface which is a "model" of the potential field. Such a model can take the form of a uniformly stretched rubber sheet supported in an appropriate manner. It is found that the effect of an electrostatic space charge can be reproduced by applying suitably distributed pressure from beneath the rubber sheet. Since the space charge is caused by the very electrons whose motion it is intended to determine, it is necessary to employ a process of successive approximation.

A description of the apparatus by means of which the pressure is applied is followed by details of four experiments; the first three of these serve as a check on the method and apparatus used, and hence relate to problems the solutions of which have been obtained by other methods (cylindrically shaped rubber sheet, Pierce electron gun, diode with thermal velocity distribution of the electrons).

The fourth experiment concerns the motion of electrons in a micro-wave valve. Two simple mathematical examples (plane diode, tetrode) demonstrating the speed of convergence of the results obtained by successive approximation are given in the appendix.

[12]) If endeavours be made to increase j beyond j_{max} the potential minimum drops to zero and electrons then commence to return from this minimum, so that the condition $\varrho = j/v$ mentioned in (7) is no longer met. The matter is dealt with fully in the book referred to in footnote [11]) (p. 40).